This article is published as part of the *Dalton Transactions* themed issue entitled:

Dalton Discussion 12: Catalytic C-H and C-X Bond Activation

Published in issue 43, 2010 of *Dalton Transactions*

Read about the Dalton Discussion 12 meeting on the *Dalton Transactions* Blog

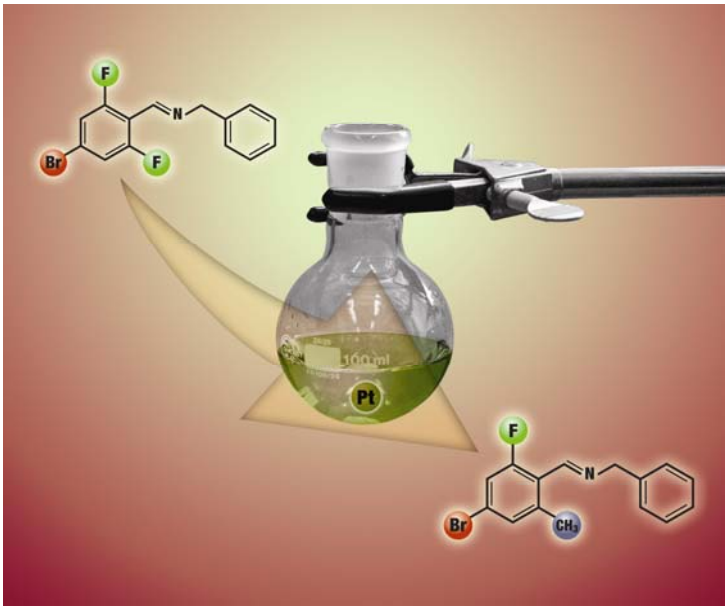

Image reproduced with the permission of Jennifer Love

Articles in the issue include:

PERSPECTIVES:

Arylation of unactivated arenes
Aiwen Lei, Wei Liu, Chao Liu and Mao Chen
Dalton Trans., 2010, DOI: 10.1039/C0DT00486C

The mechanism of the modified Ullmann reaction
Elena Sperotto, Gerard P. M. van Klink, Gerard van Koten and Johannes G. de Vries
Dalton Trans., 2010, DOI: 10.1039/C0DT00674B

Cross coupling reactions of polyfluoroarenes via C–F activation
Alex D. Sun and Jennifer A. Love
Dalton Trans., 2010, DOI: 10.1039/C0DT00540A

HOT ARTICLE:

The unexpected role of pyridine-2-carboxylic acid in manganese based oxidation catalysis with pyridin-2-yl based ligands
Dirk Pijper, Pattama Saisaha, Johannes W. de Boer, Rob Hoen, Christian Smit, Auke Meetsma, Ronald Hage, Ruben P. van Summeren, Paul L. Alsters, Ben L. Feringa and Wesley R. Browne
Dalton Trans., 2010, DOI: 10.1039/C0DT00452A

Visit the *Dalton Transactions* website for more cutting-edge inorganic and organometallic research
www.rsc.org/dalton

Synthesis, structure, and reductive elimination in the series $Tp'Rh(PR_3)(Ar^F)H$; Determination of rhodium–carbon bond energies of fluoroaryl substituents†‡

Taro Tanabe,[a] William W. Brennessel,[a] Eric Clot,[b] Odile Eisenstein[b] and William D. Jones*[a]

Received 17th March 2010, Accepted 8th June 2010
DOI: 10.1039/c0dt00157k

A series of complexes of the type $Tp'Rh(PR_3)(Ar^F)H$, where $PR_3 = PMe_3$ (**3**) and PMe_2Ph (**9**), $Ar^F = C_6F_5$ (**a**), 2,3,4,5-C_6F_4H (**b**), 2,3,5,6-C_6F_4H (**c**), 2,4,6-$C_6F_3H_2$ (**d**), 2,3-$C_6F_2H_3$ (**e**), 2,5-$C_6F_2H_3$ (**g**), and 2-C_6FH_4 (**h**) and Tp′ = tris(3,5-dimethylpyrazolyl)borate, has been synthesized as stable crystalline compounds by the reactions of the $[Tp'Rh(PR_3)]$ fragment with the corresponding fluorinated aromatic hydrocarbons, and their structures were characterized by NMR spectroscopy and elemental analysis together with X-ray crystallography. The kinetics of the reductive eliminations of fluoroarenes from complexes **3a–h** in benzene-d_6 solutions at 140 °C were investigated, but were complicated by the formation of the rhodium(I) bisphosphine complex, $Tp'Rh(PMe_3)_2$ (**4**). On the other hand, thermal reactions of (**9**) in THF-d_8 solutions at 120 °C resulted in the formation of an intramolecular C–H bond activated complex of the phenyl group on the phosphorus atom, $Tp'Rh(\kappa^2\text{-}C_6H_4\text{-}2\text{-}PMe_2)H$ (**7**), which prevents the formation of the corresponding bisphosphine complex. The experimentally determined rates of the reductive eliminations of fluoroarenes from the complexes **9a–h** and their kinetic selectivities for formation in competition with the metallacycle have been used to determine relative $Rh–CAr^F$ bond energies. The $Rh–CAr^F$ bond energy is found to be dependent on the number of *ortho* fluorines. A plot of $Rh–CAr^F$ *vs.* C–H bond strengths resulted in a line with a slope $R^{M–C/C–H}$ of 2.15 that closely matches the DFT calculated value (slope = 2.05).

Introduction

The activation and functionalization of C–H bonds of hydrocarbons for industrial and synthetic processes utilizing homogeneous transition metal catalysts has been one of the most attractive subjects in organometallic chemistry, and has been widely studied from the viewpoint of not only fundamental chemistry but also their application towards organic synthesis and material science.[1] To understand the kinetic and thermodynamic selectivity of C–H bond activation, several useful transition metal systems have been developed which are capable of activation of aromatic and aliphatic C–H bonds in homogeneous solution.[1–7]

Some of these transition metal complexes contain metals in high oxidation states and act through an electrophilic σ-metathesis pathway,[2] while others are in low oxidation states and react by oxidative addition of the C–H bond.[3] Focusing on rhodium metal systems of the latter variety, the 16 electron coordinatively unsaturated metal fragments $[Cp^*Rh(PMe_3)]$,[4] $[Tp'Rh(CO)]$[5] or $[Tp'Rh(CNCH_2CMe_3)]$[6] (Cp* = C_5Me_5, Tp′ = tris(3,5-dimethylpyrazolyl)borate), generated by the photolysis of $Cp^*Rh(PMe_3)H_2$, $Tp'Rh(CO)_2$ or $Tp'Rh(CNCH_2CMe_3)(\eta^2\text{-}PhN{=}C{=}NCH_2CMe_3)$ respectively, have been well studied mechanistically in detail.[1,7]

In the past few decades, much attention has been focused on correlations between metal–carbon and carbon–hydrogen bond strengths by utilizing such transition metal systems, and only a limited number of experimental correlations have been reported so far.[6,8–14] On the other hand, remarkable progress has been made in the *catalytic* C–H bond activation of benzene derivatives, especially by borylation[15] or by direct arylation.[16] A wide range of functionalized benzene derivatives has also been investigated in the past decade, including fluorinated aromatic hydrocarbons,[17] which offer the possibility for both C–H and C–F bond activation.[18]

Perutz *et al.* have found that $[Cp^*Re(CO)_2]$ was capable of C–H bond activation of partially fluorinated aromatic hydrocarbons,[19] while previously reported nickel complexes, such as $[Ni(PEt_3)_2]$, [Ni(dtbpe)] or $[Ni((i\text{-}Pr)_2Im)_2]$ (dtbpe = $(t\text{-}Bu)_2PCH_2CH_2P(t\text{-}Bu)_2$, $(i\text{-}Pr)_2Im$ = 1,3-di(isopropyl)imidazol-2-ylidene), were found to be favorable to C–F bond activation.[20] They demonstrated the relationship between M–C and C–H bond energies and revealed that *ortho* fluorine substitution produces a much larger increase in the M–C over the C–H bond energy, both by theoretical and experimental approaches.[19,21] Furthermore, Perutz and Eisenstein *et al.* reported exciting results that the number of *ortho* fluorine substituents strongly affected the M–C bond strength while the *total* number of fluorine substituents only had a minor effect on the M–C bond strength.[21,22] Complexes with two *ortho* fluorines had calculated M–C bond strengths ~5 kcal mol^{-1} higher

[a]*Department of Chemistry, University of Rochester, Rochester, New York, 14627, USA. E-mail: jones@chem.rochester.edu*
[b]*Institut Charles Gerhardt, Université Montpellier 2, CNRS 5253, case courrier 1501, Place E., Bataillon, 34095, Montpellier, France*

† Based on the presentation given at Dalton Discussion No. 12, 13–15th September 2010, Durham University, UK.

‡ Electronic supplementary information (ESI) available: Detailed results of the kinetics of the reductive eliminations, coordinates and energies for calculated complexes, a summary of the calculation procedure, the full list of authors for reference 38, and summaries of structural refinements. CCDC reference numbers for **1**, **2-*d*$_6$**, **3a**, **3b**, **3d**, **3g**, $Tp'RhCl_2(PPhMe_2)$, **5**, **7**, **9a**, **9b**, **9c**, **9d**, **9e** and **9g**: 770109–770123. For ESI and crystallographic data in CIF or other electronic format see DOI: 10.1039/c0dt00157k

than complexes with one *ortho* fluorine in the aryl ligand of $Cp^*Re(CO)_2Ar^FH$.

Very recently, we have also independently reported the experimental and theoretical correlation of the Rh–C bond strength of fluoroaryls, using the system $Tp'Rh(CNCH_2CMe_3)(Ar^F)H$. The M–C bond strength is also strongly dependent on the number of *ortho* fluorine substituents and only mildly dependent on the *total* number of fluorine substituents on the phenyl ring.[23] Complexes with aryl groups containing two *ortho* fluorine substituents have barriers to reductive elimination that are ~5 kcal mol^{-1} higher than those for a single *ortho* fluorine substituent.[23] Furthermore, the relationship between Rh–C_{Ar} and C–H bond strengths for a series of these complexes has been found to be linear (slope = 2.14), and closely matched the theoretically calculated value (slope = 1.96).[23] Complexes bearing electron withdrawing (π accepting character) ligands, such as CO and RNC, have been used in these systems. Eisenstein *et al.* have reported theoretical results[22] that indicate that the change in the nature of the spectator ligands affects the value of the slope $R^{M\text{–}C/C\text{–}H}$ and their selectivities. We have prepared a series of stable crystalline compounds $Tp'Rh(PR_3)(Ar^F)H$ (PR_3 = PMe_3 (**3**) and $PPhMe_2$ (**9**); Ar^F = C_6F_5 (**a**), 2,3,4,5-C_6F_4H (**b**), 2,3,5,6-C_6F_4H (**c**), 2,4,6-$C_6F_3H_2$ (**d**), 2,3-$C_6F_2H_3$ (**e**), 2,5-$C_6F_2H_3$ (**g**), and 2-C_6FH_4 (**h**)) by the reactions of a $[Tp'Rh(PR_3)]$ fragment with fluorinated benzene derivatives, and their structures were characterized by NMR spectroscopy together with X-ray crystallography. Experimental results employing kinetic techniques have been used to relate the Rh–CAr^F *vs.* C–H bond strengths, and the relative free energies of these phosphine coordinated complexes will be described.

Results and discussion

Synthesis of $Tp'Rh(PMe_3)Ar^FH$ (3)

The rhodium dihydride complex bearing Tp′ and trimethylphosphine ligands, $Tp'RhH_2(PMe_3)$ **1**, is known to be an excellent precursor of rhodium(I) fragment $[Tp'Rh(PMe_3)]$ under near-UV irradiation. Although Carmona *et al.*,[24] and more recently our group[25] have reported the synthesis and spectroscopic data of **1**, there have been no reports on its crystal structure (Scheme 1). Recrystallization of **1** from hexane afforded colorless crystals and the molecular structure was revealed by X-ray structural analysis (Fig. 1). A slightly distorted octahedral geometry around the rhodium metal center was observed. The rhodium–nitrogen (for Tp′) bond lengths (2.2193(13), 2.1124(11) and 2.2076(12) Å) are slightly longer than those of the corresponding rhodium dichloride derivative (2.151(2), 2.087(2) and 2.145(2) Å).[26]

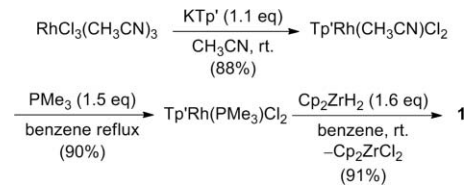

Scheme 1 Synthesis of rhodium dihydride **1**.

Complete conversion of **1** to $Tp'Rh(PMe_3)(C_6H(D)_5)H(D)$ (**2** or **2-*d*$_6$**) was accomplished by photolysis of **1** (λ = 304 nm, ε = 165 cm^{-1} M^{-1}) in C_6H_6 or C_6D_6 with light from a Hg/Xe lamp that had been filtered using a 270–370 nm band pass filter. Similarly, C–H bond activated products of the fluorobenzenes, $Tp'Rh(PMe_3)(Ar^F)H$ (**3a–h**), have been synthesized and isolated as stable crystalline compounds by the irradiation of **1** in the corresponding fluorobenzene solution as shown in Scheme 2. Only a single isomer of the fluorobenzene activated product was obtained in the synthesis of **3a–d** and **3g**. On the other hand, in the synthesis of **3e** (1,2-difluorobenzene), **3f** (1,3-difluorobenzene), and **3h** (fluorobenzene), two or three isomers were obtained upon irradiation.

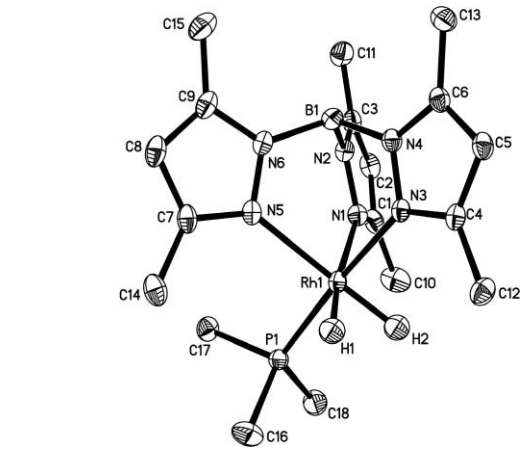

Fig. 1 X-ray structure of **1** (thermal elipsoids at 50% probability level). Hydrogen atoms except for RhH_2 were omitted for clarity.

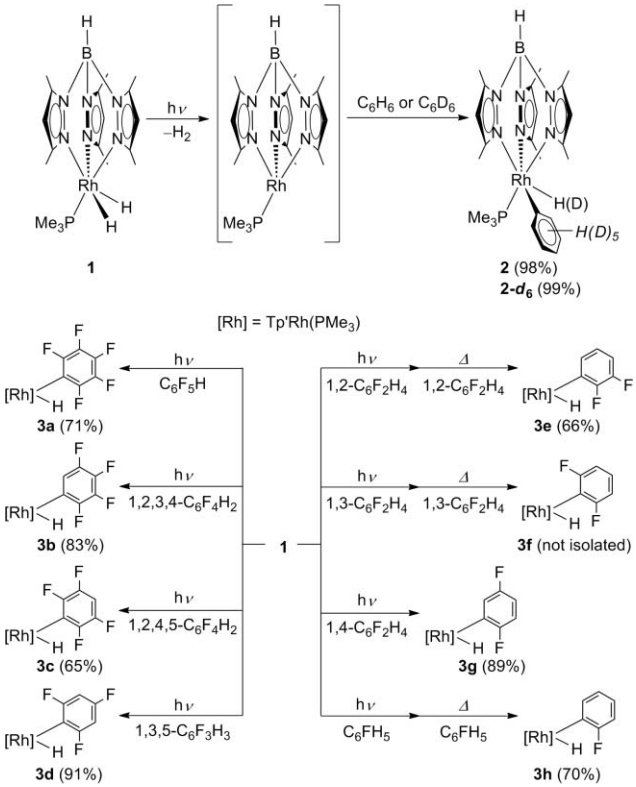

Scheme 2 Synthesis of C–H bond activated products of fluorinated benzene derivatives **3** by using **1**.

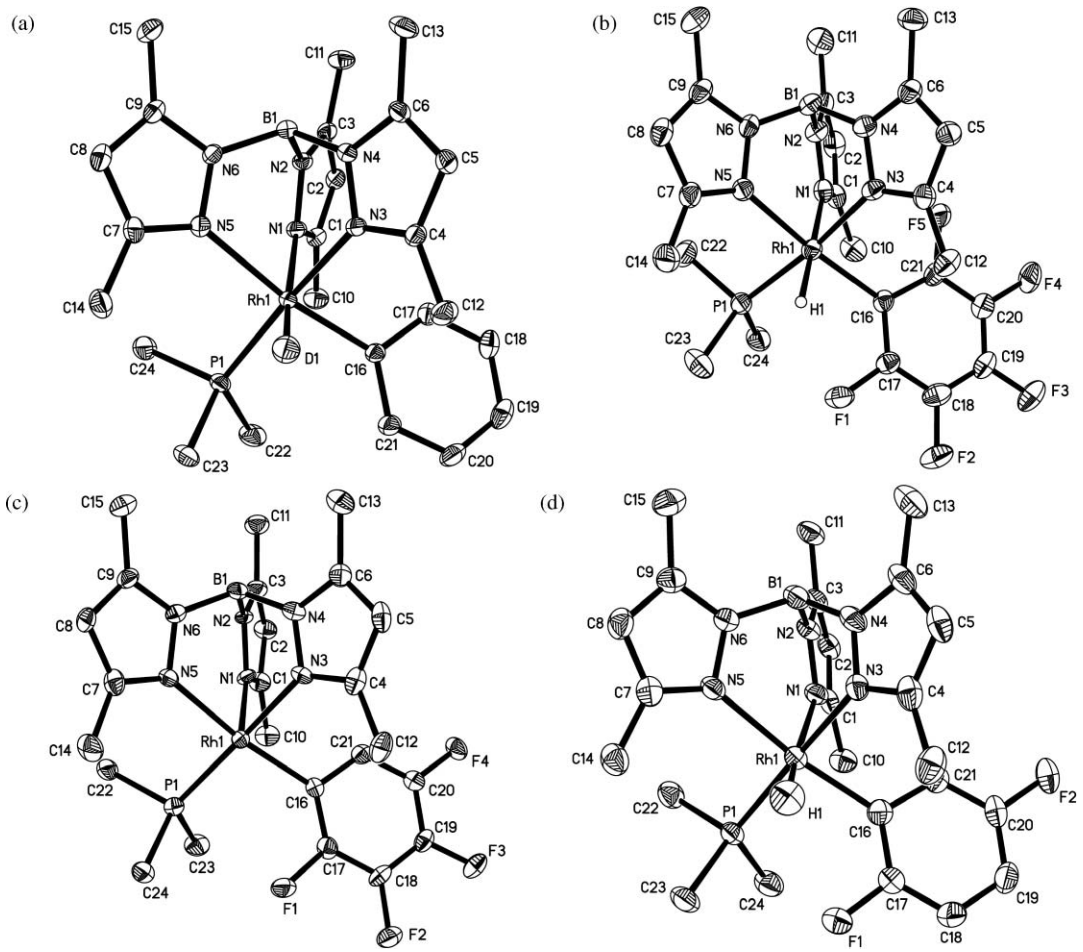

Fig. 2 X-ray structures of **2-*d*$_6$**, **3a**, **3b**, and **3g** (thermal ellipsoids at 50% probability level). Hydrogen atoms except for RhH(D) were omitted for clarity.

Heating of these crude mixtures containing isomers at 100 °C resulted in the conversion to the thermodynamically preferred products, **3e** and **3h**. However, isolation of **3f** was unsuccessful even following heating at 100 °C for three months, as a mixture of the 2,6-difluorophenyl- (**3f**), 2,4-difluorophenyl-, and 3,5-difluorophenyl- substituted complexes remained. The molecular structures of these newly isolated complexes were characterized by ^{1}H, ^{13}C{^{1}H}, ^{19}F{^{1}H} and ^{31}P{^{1}H} NMR spectroscopy together with elemental analysis. In all cases, a signal for the hydride was observed as a doublet of doublet of doublets or a doublet of triplets between δ −15 and −17 ppm. Both ^{1}H and ^{19}F{^{1}H} NMR spectra indicated hindered rotation around the rhodium–carbon(aryl) bond. For example, five inequivalent signals were observed in the case of **3a** in the ^{19}F{^{1}H} NMR spectrum. The molecular structures of the complexes, **2-*d*$_6$**, **3a**, **3b**, and **3g** were determined by X-ray crystallographic analysis (Fig. 2a–d).

In each case, similar structures were observed around the rhodium metal center showing a slightly distorted octahedral geometry. The (fluoro)aryl groups interdigitate with the pyrazolylborate groups, with the plane of the aryl group containing the three fold Rh–B axis. In the structures of **3a**, **3b** and **3g**, one of the *ortho* fluorine atoms is in close proximity to the hydride suggesting the possibility for coupling to the hydride in these cases.[23] Despite the fact that *ortho* fluorine substituent(s) on the phenyl group are known to strengthen metal–carbon(aryl) bonds due to their inductive effect, a longer Rh–Ar bond length, and wide ∠P–Rh–Ar bond angles were observed in the crystal structure of **3a** (2.046(7) Å, 96.8(2)°) compared to **2-*d*$_6$** (2.0171(15) Å, 91.06(4)°), **3b** (2.030(5) Å, 93.88(14)°), and **3g** (2.013(4) Å, 92.88(11)°). The slightly shorter Rh–Ar bond length in **3g** compared to **2-*d*$_6$** can be explained by the inductive effect of fluorine atoms. However, it should be noted that the steric repulsion around the rhodium has a more pronounced influence on the Rh–Ar^{F} bond lengths over the inductive effects of the fluorines.

Reductive elimination of fluoroarenes from 3

Reductive elimination of C_6H_6 from **2** in C_6D_6 at 100 °C has been previously reported, and follows first order kinetics with a rate constant of 8.3(1.2) × 10^{-5} s^{-1}.[25] The electron donating phosphine ligand is expected to stabilize the rhodium(III) phenyl hydride better than an electron withdrawing ligand such as CO or RNC. However, the rate constant for reductive elimination of C_6H_6 from the complex Tp′Rh(CNCH$_2$CMe$_3$)(Ph)H in C_6D_6 at 100 °C has been determined (5.4(2) × 10^{-5} s^{-1}),[6] which is slightly *smaller* than that of **2**. Rate constants for the reductive elimination of fluoroarenes from **3** (Scheme 3) were obtained in a similar way, but higher temperatures were required as compared to **2** (C_6D_6 at 140 °C in a sealed NMR tube). A plot of ln([C]$_t$/[C]$_0$) of the fluoroarene activated complex *vs.* time was used to determine the

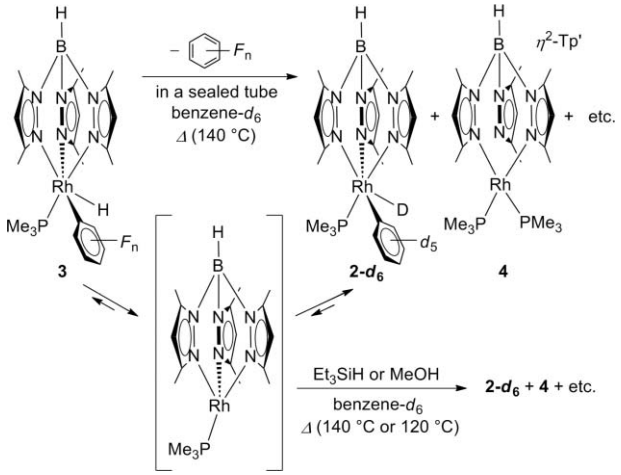

Scheme 3 Reductive eliminations of fluoroarenes from **3** in C_6D_6.

rates of the reductive eliminations. However, in all cases, a fast decrease of the integrations for hydride of **3** and the formation of rhodium(I) bisphosphine complex Tp′Rh(PMe_3)$_2$ (**4**, $\delta_P = -2.2$, $^1J_{RhP} = 171$ Hz) was observed during the reactions. Observation of a doublet signal bearing a larger value of $^1J_{RhP}$ unambiguously indicated the formation of **4**.[27] The formation of **4** prevented determination of the kinetic parameters for the reductive eliminations because the second trimethylphosphine ligand in the bisphosphine complex **4** came from decomposition of starting material **3** or product **2-*d*$_6$**. Thermal reactions of **2-*d*$_6$** in C_6D_6 were examined at 140, 120 and 100 °C. Formation of bisphosphine complex **4** was observed above 120 °C. Although thermal reaction at 100 °C suggested the possibility of determining the kinetic parameters for the reductive eliminations of complexes **3**, it would take too long (months) to determine the rates for the pentafluoro (**3a**) or 2,3,5,6-tetrafluoro (**3c**) systems bearing strong Rh–Ar^F bonds. To prevent the formation of bisphosphine complex, the thermal reactions of **2-*d*$_6$** in the presence of Et_3SiH or MeOH as trapping reagents for the rhodium(I) species [Tp′Rh(PMe_3)] were investigated. However, the formation of **4** was still observed even with these additives. These reactions afforded rhodium dihydride **1** together with **4** and an unknown species, indicating that the PMe_3 complexes are not well suited to kinetic investigations.

Intramolecular C–H bond activation of [Tp′Rh(PPhMe$_2$)]

Because of the undesirable formation of **4**, a change in the phosphine ligand of the starting material was required for further kinetic investigations. Our second choice of phosphine ligand was dimethylphenylphosphine, for two reasons: (1) to decrease the σ-donating character (minor change); (2) to introduce reactive *ortho* C–H bonds of the phenyl group on the phosphorus atom to trap the rhodium(I) metal center. Although triphenylphosphine was also considered for prevention of the formation of the bisphosphine complex, it has substantial π-accepting character together with weak σ-donating character. Instead, the rhodium dihydride bearing dimethylphenylphosphine, Tp′RhH_2(PPhMe$_2$) **5**,[24] was prepared by the same method used for **1** with a similar yield. The molecular structure of **5** was revealed by X-ray crystallography (Fig. 3). The rhodium–nitrogen bond lengths (2.2341(18), 2.1036(18) and 2.1863(18) Å) were similar to those

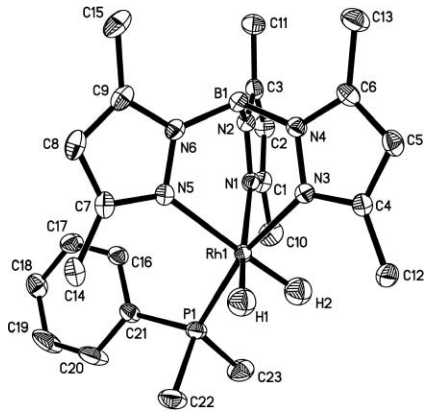

Fig. 3 X-ray structure of **5** (thermal ellipsoids at 50% probability level). Hydrogen atoms except for RhH_2 were omitted for clarity.

seen in **1**, and the rhodium–phosphorus bond length (2.2218(6) Å) showed a slightly longer value than that of **1** (2.2178(5) Å).

The benzene-d_6 activated product Tp′Rh(C_6D_5)D(PPhMe$_2$) **6-*d*$_6$** was prepared by the irradiation of **5** in C_6D_6 in 64% isolated yield. Then thermal reaction of **6-*d*$_6$** in C_6D_6 was examined at 120 °C. Reaction for 3 h afforded the four-membered-ring rhodacycle, which possesses an intramolecular orthometallated C–H bond activated phenyl group, Tp′Rh(κ^2-C_6H_4-2-PMe$_2$)H (**7**). **7** forms in about 25% yield as judged by ^{1}H NMR spectroscopy (Scheme 4). No change of the ratio of **7** to **6-*d*$_6$** (1 : 3) was observed with heating at 120 °C for 1 day or more. It should be noted that less than 1% of the corresponding bisphosphine complex, Tp′Rh(PhMe$_2$)$_2$ **8**, was observed.[27] No other species except for **7** and **6-*d*$_6$** could be detected in the ^{1}H NMR spectrum during the reaction. Furthermore, these results suggested an equilibrium between **7** and **6-*d*$_6$** in C_6D_6. Changing the solvent for this mixture from C_6D_6 to THF followed by the heating at 120 °C for 1 h resulted in the quantitative conversion to **7**, which was isolated in 84% yield (Scheme 4) and characterized by NMR spectroscopy together with elemental analysis. Observation of four protons assignable to the phenyl ring in the aromatic region of the ^{1}H

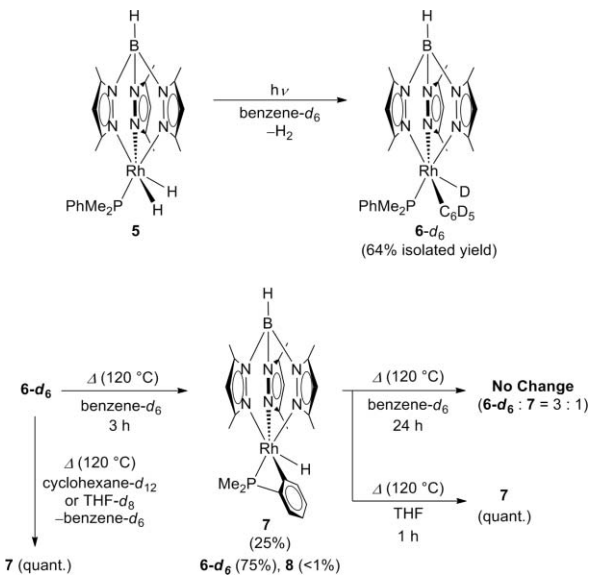

Scheme 4 Synthesis and thermal reactions of **6-*d*$_6$**.

NMR spectrum and a high field ^{31}P shift compared with that of **6-d_6** (**7**: $\delta_P = -65.12$; **6-d_6** $\delta_P = 15.35$) strongly suggested the cyclometallated structure of **7**.[28] The molecular structure of **7** was unambiguously determined by X-ray structural analysis (Fig. 4).

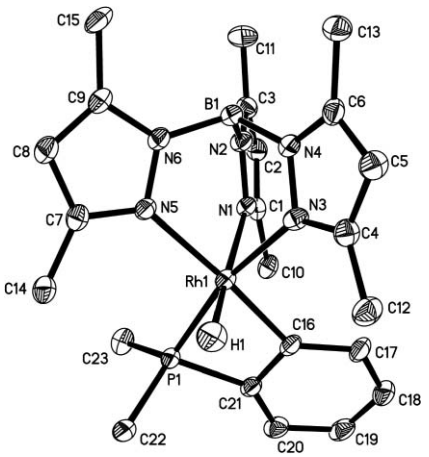

Fig. 4 X-ray structure of **7** (thermal ellipsoid plot with 50% probability level). Hydrogen atoms except for RhH were omitted for clarity.

The results shown in Scheme 4 suggested that it would be possible to measure the rates for the reductive eliminations of fluoroarenes in these complexes without any additional trapping reagents (the Rh(I) species traps itself by cyclometallation). Although conversion of Rh(I) to the four-membered-ring rhodacycle **7** should be reversible (equilibrium), fast intramolecular C–H insertion was found to prevent the formation of bisphosphine complex **8**.

Synthesis and kinetic selectivities of Tp′Rh(PhMe$_2$)Ar^{F}H (9)

The isolated yield of **6-d_6** (64%) is significantly lower than that of **2-d_6** (99%). In the synthesis of **6-d_6**, intramolecular C–H bond activated product **7** was also obtained after the photo-irradiation (**6-d_6** : **7** = 6.7 : 1.0). Heating the C_6D_6 solution of the crude mixture followed by purification afforded **6-d_6** in pure form. Employing similar reactions as for **3a–h**, the C–H bond activated products Tp′Rh(PhMe$_2$)(Ar^F)H (**9a–h**) have been synthesized and isolated as stable crystalline compounds as shown in Scheme 5. As before, it should be noted that heating in the corresponding fluoroarene solvent after the irradiation is necessary to obtain the products in good yields because of the kinetically competitive formation of **7**. These complexes were characterized by ^1H, $^{13}C\{^1H\}$, $^{31}P\{^1H\}$ and $^{19}F\{^1H\}$ NMR spectroscopy together with elemental analysis.

The relative free energy values (ΔG°) for the fluorobenzene oxidative addition products **9** can be determined by analysis of the kinetics for fluoroarene reductive elimination ($\Delta G^\ddagger_{re}$) together with the kinetic selectivities ($\Delta\Delta G^\ddagger_{oa}(Ar^FH)$) according to eqn 1. The kinetic selectivities ($\Delta\Delta G^\ddagger_{oa}(Ar^FH)$) of the fluorobenzene activated product **9** and cyclometallated product **7** can be directly estimated based on the ratio with intramolecular C–H bond activated product **7** just after irradiation as measured by ^1H NMR spectroscopy, as shown in Schemes 6 and 7, eqn 2, and graphically in Fig. 5. Basically, $\Delta\Delta G^\ddagger_{oa}(Ar^FH)$ in this system are shown as the kinetic selectivities for each (fluoro)benzene activated compound **6** or **9** as compared with that of cyclometallated compound **7**.

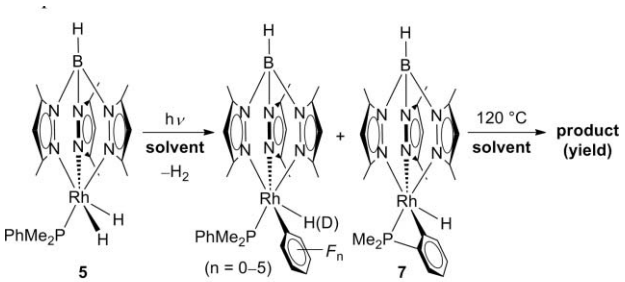

solvent	Ar$^{(F)}$	product	yield[a]
C_6H_6	C_6H_5	**6**	70%
C_6D_6	C_6D_5	**6-d_6**	68%
C_6F_5H	C_6F_5	**9a**	82%
1,2,3,4-$C_6F_4H_2$	2,3,4,5-C_6F_4H	**9b**	79%
1,2,4,5-$C_6F_4H_2$	2,3,5,6-C_6F_4H	**9c**	76%
1,3,5-$C_6F_3H_3$	2,4,6-$C_6F_3H_2$	**9d**	85%
1,2-$C_6F_2H_4$	2,3-$C_6F_2H_3$	**9e**	89%
1,3-$C_6F_2H_4$	2,6-$C_6F_2H_3$	**9f**	not isolated[b]
1,4-$C_6F_2H_4$	2,5-$C_6F_2H_3$	**9g**	91%
C_6FH_5	2-C_6FH_4	**9h**	85%

a: isolated yield; *b*: after heating for 1 month, mixture with 2,4-$C_6F_2H_3$- and 3,5-$C_6F_2H_3$-substituted isomers was obtained.

Scheme 5 Synthesis of C–H bond activated products of fluorinated benzene derivatives **9** by utilizing **5**

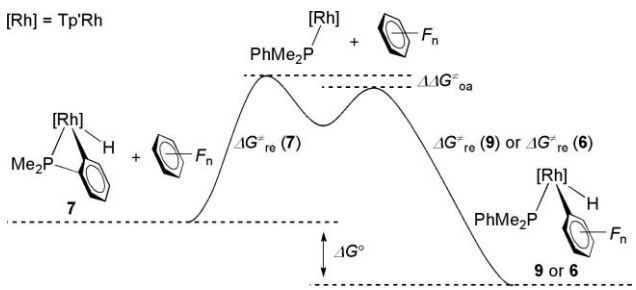

Fig. 5 Free energy diagram for activation of hydrocarbon C–H bonds with [Tp′Rh(PPhMe$_2$)].

$$\Delta G^\circ = \Delta G_{re}(\mathbf{7}) - \Delta\Delta G_{oa}(Ar^FH) - \Delta G_{re}(\mathbf{9}\text{ or }\mathbf{6}) \quad (1)$$

$$\Delta\Delta G_{oa}(Ar^FH) = RT\ \ln([\mathbf{9}\text{ or }\mathbf{6}]/[\mathbf{7}]) \quad (2)$$

Scheme 6 shows the kinetic selectivities as the ratio of **9a–g** (or **6**) to **7** just after irradiation. In these six systems, a single isomer of the fluorobenzene (or benzene) activated product was obtained after the photolysis. In the synthesis of **9a** and **9b**, the ratio of **9** to **7** was almost 1 : 2 in the pentafluoro system (**9a**), while the ratio was 2 : 1 in the 1,2,3,4-tetrafluoro system (**9b**). On the other hand, both **9c** and **9d** were formed in almost equal amounts compared to **7**. **9g** and **6** showed the largest selectivities relative to **7**. Scheme 7 shows the ratio of **9e** or **9h** *vs.* **7** in the reactions with 1,2-difluorobenzene or fluorobenzene. These systems afforded two or three isomers with kinetic selectivities comparable to the other mono *ortho*-fluoro aryl products. The mild selectivities result in small values for $\Delta\Delta G^\ddagger_{oa}(Ar^FH)$, in which the largest difference observed was between **9a** ($\Delta\Delta G^\ddagger_{oa} = -0.40$ kcal mol^{-1}) and **6** ($\Delta\Delta G^\ddagger_{oa} = +1.12$ kcal mol^{-1}).

The molecular structures of these newly isolated complexes, **9a**, **9b**, **9c**, **9d**, **9e** and **9g**, were unambiguously revealed by X-ray crystallographic analysis. Similar to the complexes **3** bearing

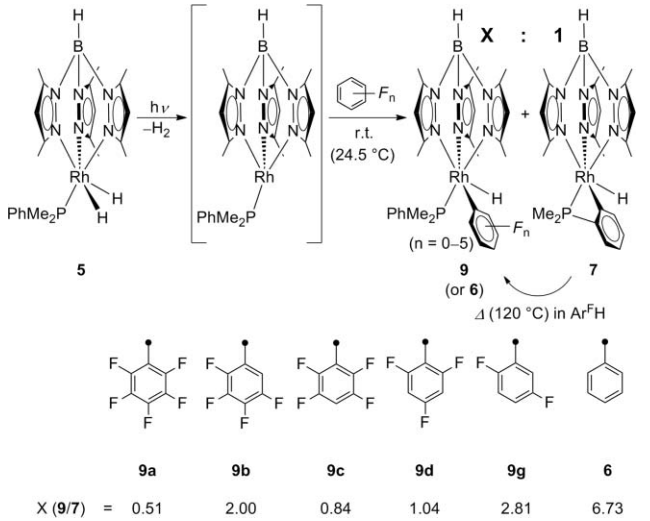

Scheme 6 The ratio of the fluoroarene activated product based on **7** after photo-irradiation in the synthesis of **9a–d**, **9g** and **6**.

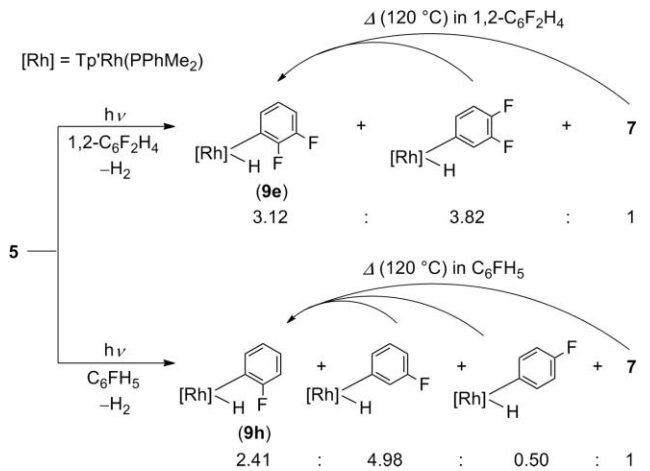

Scheme 7 The ratio of the fluoroarene activated product based on **7** after photo-irradiation in the synthesis of **9e** and **9h**.

a PMe_3 ligand, slightly distorted octahedral geometries around the rhodium metal center are also observed in these complexes (Fig. 6a–f). It should be noted that the phenyl group on the phosphorus atom is oriented away from the rhodium metal center in these complexes. As observed in the PMe_3 system, the observed length of the Rh–Ar^F bond of **9a** (2.0400(10) Å) was longer than those in **9b** (2.0228(11) Å), **9e** (2.028(4) Å) and **9g** (2.0329(16) Å) (bearing one *ortho* fluorine) because of steric repulsion, and very similar to those of **9c** (2.0388(17) Å) and **9d** (2.0446(13) Å) (bearing two *ortho* fluorines). The steric repulsion around the rhodium still has a critical influence on the rhodium–carbon bond lengths as does the inductive effects of fluorine substituents in the structures. As with the PMe_3 complexes, some of the aryl carbons in compounds **9** could not be observed in their $^{13}C\{^1H\}$ NMR spectra because of the multiple couplings with many of the fluorines in the aryl group.

The structural features of **9** can be compared with those of intramolecular C–H bond activated product **7**. The Rh–Ar^F bond lengths of **9** were slightly longer than that of **7** (2.022(5) Å), probably because of the steric repulsion in **9** that is absent in **7**. The ^1J rhodium–phosphorus coupling constant of **7** (114 Hz) in the $^{31}P\{^1H\}$ NMR spectrum was much smaller than those of **9** (132–136 Hz) by almost 20 Hz. However, the rhodium–phosphorus bond length of **7** (2.2468(15) Å) was shorter than those of **9** (**9a**: 2.2777(3) Å; **9b**: 2.2649(4) Å; **9c**: 2.2643(5) Å; **9d**: 2.2688(4) Å; **9e**: 2.2545(10) Å; **9g**: 2.2681(5) Å).

Reductive eliminations of fluoroarenes from 9

The rates of reductive elimination of fluoroarenes from complexes **9a–e**, **9g–h**, and **6** were determined at 120 °C in THF-d_8 by monitoring the conversion of the complexes to **7** by ^1H NMR spectroscopy (Scheme 8). Kinetic analysis was performed by integration of the decreasing hydride resonance relative to an internal standard by ^1H NMR spectroscopy. A first order plot of the decay of the concentration of **9** or **6** *vs.* time showed upward curvature, as the reactions did not go to completion but rather approached equilibrium (71–98% complete). Therefore, the rate of Ar^FH reductive elimination (k_1) from **9** was determined by a kinetic simulation of eqn 3 using the KINSIM/FITSIM software package (see Supporting Information for details‡).[29]

$$9 \underset{k_{-1}}{\overset{k_1}{\rightleftharpoons}} 7 \qquad (3)$$

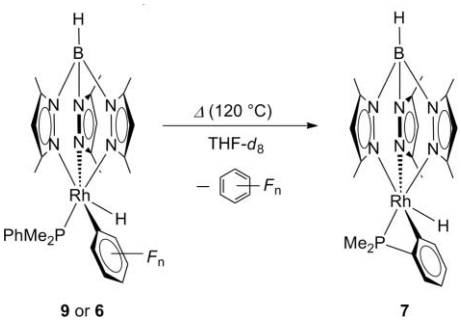

Scheme 8 Kinetics of the reductive elimination of fluoroarenes from the complexes **9** and **6** at in THF-d_8.

Kinetics for the complexes **9b**, **9c**, **9d**, **9e**, **9g** and **9h** were successfully simulated using this approach to an equilibrium model. For the pentafluorobenzene activated product **9a**, however, a plot of ln[**9a**] *vs.* time showed *downward* curvature, which was attributed to slow decomposition of **7** during the long reaction time ($\tau_{\frac{1}{2}} \approx 4$ months @ 120 °C). As a result, the rate of reductive elimination af C_6F_5H from **9a** was estimated using initial rate data only (see Supporting Information‡). The rate constant reported for **9a** should therefore be considered as an upper limit and the relative free energy $\Delta G°$ as a lower limit (*vide infra*). In contrast, the reductive elimination of benzene in **6** at 120 °C was too fast to monitor by NMR spectroscopy. Therefore, this rate constant was extrapolated from an Eyring plot using rate data recorded at 60, 70, 80, and 90 °C ($\Delta H^{\neq} = 37.4 \pm 3.5$ kcal mol^{-1}; $\Delta S^{\neq} = 27 \pm 10$ e.u., see Supporting Information‡).

Table 1 summarizes the experimental results of the kinetics of reductive elimination of fluoroarenes from **9a–e**, **9g–h**, and **6**, showing rate constant $k_{re}(Ar^FH)$ along with the corresponding $\Delta G^{\neq}_{re}$ activation energies. As expected, the observed $\Delta G^{\neq}_{re}$ of **9a** was largest, consistent with a strong Rh–Ar^F bond. Focussing on the comparison of **9b** and **9d** in this system, the *ortho* fluorine effect

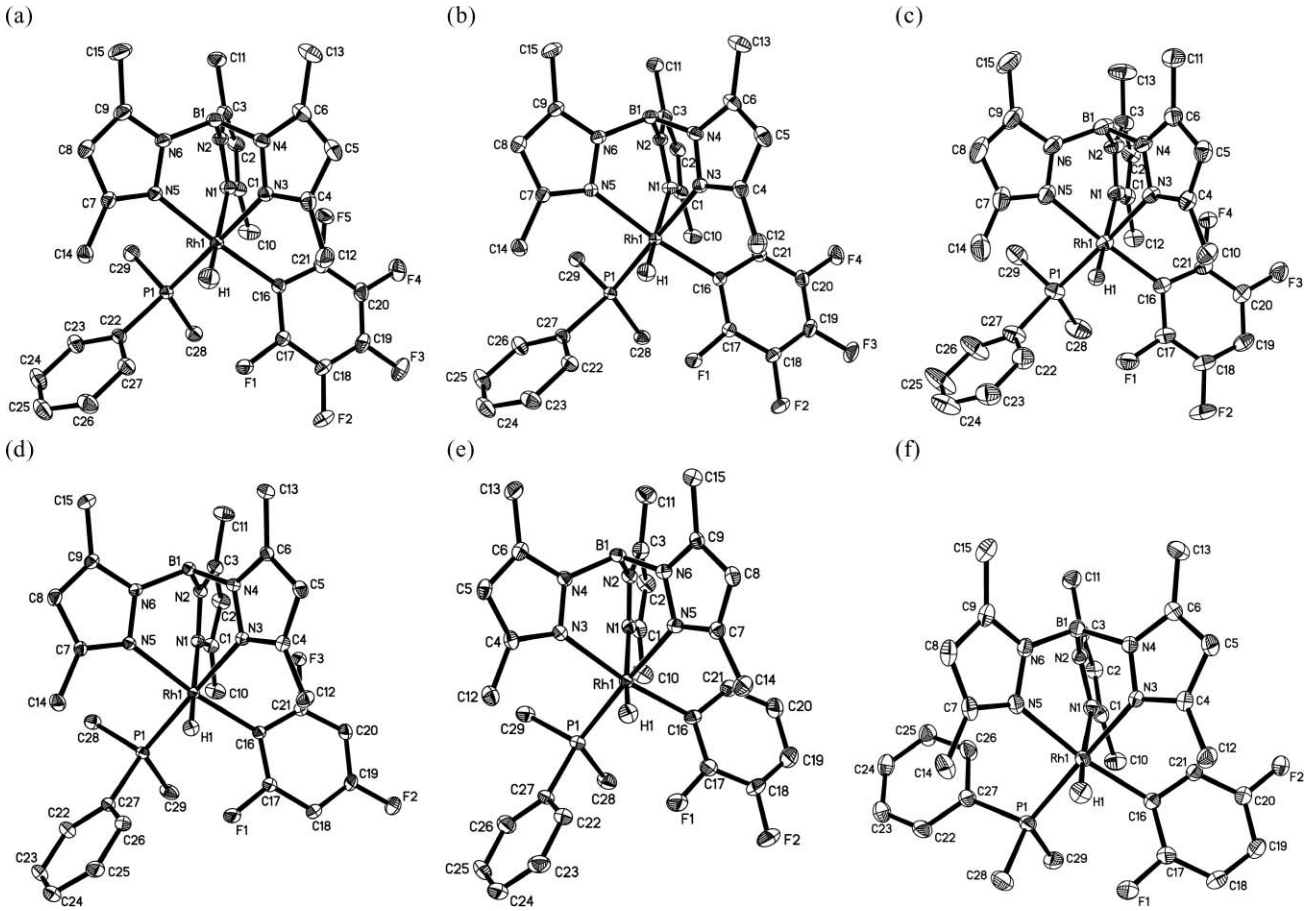

Fig. 6 X-ray structures of **9a**, **9b**, **9c**, **9d**, **9e**, and **9g** (a–f, thermal ellipsoids at 50% probability level). Hydrogen atoms except for RhH were omitted for clarity.

Table 1 Rates of reductive elimination of Ar^FH from Tp′Rh(PPhMe$_2$)-Ar^FH at 120 °C

Complex	Ar^F	$k_{re}(Ar^FH)/s^{-1}$	$\Delta G^{\neq}_{re}$/kcal mol^{-1}
9a	C_6F_5	$7.04(0.61) \times 10^{-8}$	36.09(0.07)
9b	2,3,4,5-C_6F_4H	$9.86(0.69) \times 10^{-7}$	34.03(0.05)
9c	2,3,5,6-C_6F_4H	$1.79(0.05) \times 10^{-7}$	35.37(0.02)
9d	2,4,6-$C_6F_3H_2$	$8.93(0.13) \times 10^{-6}$	32.31(0.01)
9e	2,3-$C_6F_2H_3$	$5.85(0.13) \times 10^{-5}$	30.84(0.02)
9g	2,5-$C_6F_2H_3$	$3.05(0.06) \times 10^{-5}$	31.35(0.02)
9h	2-C_6FH_4	$2.50(0.02) \times 10^{-4}$	29.71(0.01)
6[a]	C_6H_5	$1.22(0.70) \times 10^{-2}$	26.67(0.45)

[a] The rate of the reaction was measured at various lower temperatures, 60, 70, 80, and 90 °C, and the reaction rate at 120 °C estimated by the EYRING plot of ln(k/T) *vs.* 1/T. Errors are reported as standard deviations.

also has critical but not sole influence on $\Delta G^{\neq}_{re}$. For example, the $\Delta G^{\neq}_{re}$ for **9d** (total #F = 3, *ortho* #F = 2) is *lower* than that of **9b** (total #F = 4, *ortho* #F = 1), but it is still much higher than those of the difluoro species **9e** or **9g** (total #F = 2, *ortho* #F = 1).

Thermodynamics for fluoroarene C–H bond activation by [Tp′Rh(PPhMe$_2$)]: Relative Rh–C$_{Ar}$ *vs.* C–H bond strength

The thermodynamics for the fluoroarene C–H bond activation by [Tp′Rh(PPhMe$_2$)] were determined by using the results from the reductive elimination and kinetic selectivity experiments. As indicated in Fig. 5, the relative free energy value $\Delta G°$ for the complexes, **9a–e**, **9g–h**, and **6**, can be determined using eqn 1. Furthermore, using the experimentally determined $\Delta G°$ values along with calculated C–H bond strengths for each of the fluoroarenes, the relative Rh–Ar^F bond strengths in complexes **9** can be determined according to eqn 4, which includes the assumption that $\Delta G° \approx \Delta H° - RT \ln(H_9/H_7)$, where H_9/H_7 is the ratio of the number of hydrogens that can be activated on the fluoroarene substrate divided by the number of hydrogens available for activation in **7** (= 2H); *i.e.*, the $\Delta S°$ values are the same for these reactions,[6] other than the statistical contribution for the number of hydrogens. Since these experiments measure $\Delta G°$, whereas bond strengths are reflected by $\Delta H°$, a correction for $\Delta S°$ must be included.

$$D_{rel}(Rh–Ar^F) = [\Delta H(Rh–Ar^F) - \Delta H(Rh–Ar^7)] = \Delta G° - RT \ln(H_9/H_7) - [D(Ar^F–H) - D(Ar^7–H)] \quad (4)$$

Table 2 summarizes the kinetic and thermodynamic data for formation of Tp′Rh(Ar^F)H(PPhMe$_2$). The Rh–Ar^F bond strengths have been adjusted to be relative to that of the phenyl hydride complex, **6** (which is set to 0 kcal mol^{-1}), rather than to metallacycle **7**. For comparison, DFT was used to calculate Rh–Ar^F bond strengths as done previously (see Supporting Information for details‡).[30] As can be seen, the trend in the experimental data for $D(Rh–Ar^F)_{rel}$ *vs.* $D(Ar^F–H)$ is in excellent agreement with the trend

Table 2 Kinetic and thermodynamic data for formation of Tp′Rh(PPhMe$_2$)Ar^{F}H (kcal mol^{-1})

	$\Delta\Delta G_{oa}^{\neq a}$	$\Delta G_{re}^{\neq}$	$\Delta G^{\circ b}$	Calcd [c] D(Ar^F–H)	Exptl[b] [d] D(Rh–Ar^F)$_{rel}$	Calcd[bd] [e] D(Rh–Ar^F)$_{rel}$
9a	–0.40	36.09	–7.91	123.0	14.09	14.4
9b	+0.41	34.03	–6.65	120.6	10.8	10.3
9c	–0.10	35.37	–7.48	122.5	13.5	13.7
9d	+0.02	32.31	–4.55	123.2	11.1	11.8
9e	+0.67	30.84	–3.72	119.6	6.9	8.2
9g	+0.61	31.35	–4.17	119.8	7.1	8.3
9h	+0.52	29.71	–2.44	119.6	5.6	7.0
6	+1.12	26.67	0.00	117.1	0.0	0.0

[a] Relative to metallacycle (**7**). [b] Relative to phenyl hydride complex. [c] Data from Ref. 22. [d] ΔH Corrected for number of hydrogens available for activation. [e] calculated for the complexes, Tp′Rh(Pme$_3$)Ar^{F}H.

of calculated D(Rh–Ar^F)$_{rel}$ *vs.* D(Ar^F–H) for the complexes. The pentafluorobenzene activated product, **9a**, has the strongest Rh–Ar^F bond. The bond strengths in complexes containing two *ortho* fluorines exceed that in **6** by an average of about 13 kcal mol^{-1}. The bond strengths in complexes containing one *ortho* fluorine exceed that in **6** by an average of about 5 kcal mol^{-1}. As observed earlier in the system Tp′Rh(Ar^F)H(CNneopentyl)[23] bearing the electron withdrawing isonitrile ligand as a spectator ligand, the Rh–Ar^F bond strength is still strongly dependent on the number of *ortho* fluorines and only mildly dependent on the *total* number of fluorines on the phenyl ring in this system. It is interesting to compare bond strengths in the 1,2,3,4-tetrafluorobenzene (**9b**, one *ortho* fluorine) and 1,3,5-trifluorobenzene (**9d**, two *ortho* fluorines) activated complexes. In the phosphine system examined here, both by experiment and DFT calculation, the difference in the D(Rh–Ar^F)$_{rel}$ values was much smaller (0.3 kcal mol^{-1}) than the corresponding difference in the isonitrile system (3.3 kcal mol^{-1}). This result indicates that the total number of fluorines plays a more significant role in the phosphine containing system compared with the isonitrile system.

A plot of theoretically calculated C–H bond strengths D(Ar^F–H) *vs.* experimentally determined Rh–Ar^F bond strengths D(Rh–Ar^F) shows an almost linear correlation with a slope of 2.15 (Fig. 7a). In addition, this plot closely matches with the theoretically calculated plot (slope = 2.05, Fig. 7b), indicating that DFT can be used to accurately model these thermodynamics. The strong similarity between these plots implies that there is also a strong correlation between D(Rh–Ar^F)^{expt} and D(Rh–Ar^F)^{calc} (see Supporting Information‡). Furthermore, these results indicate that the effect of *ortho*-fluorine on the strength of the Rh–Ar^F bond is substantial, as concluded in the previously examined systems Cp*Re(Ar^F)H(CO)$_2$ (slope = 2.25)[19] and Tp′Rh(Ar^F)H(CNneopentyl) (slope = 2.14).[23]

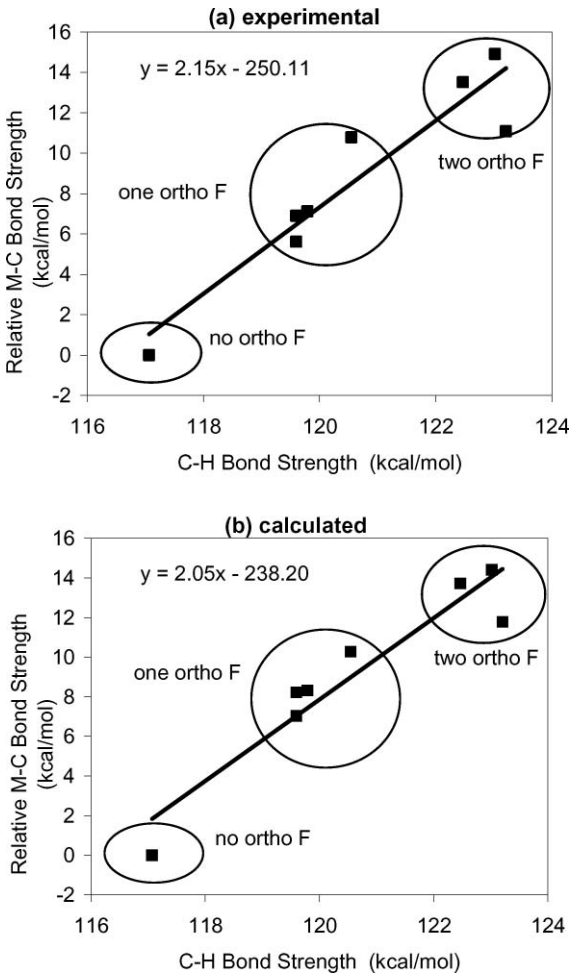

Fig. 7 Plot of relative Rh–Ar^F bond strength *vs.* calculated C–H bond strength (kcal mol^{-1}); Experimental result (a) and DFT calculated result (b).

Conclusions

We have succeeded in the synthesis and isolation of the series of complexes of the type Tp′Rh(PR$_3$)(Ar^F)H, where PR$_3$ = PMe$_3$ (**3**) and PMe$_2$Ph (**9**), Ar^F = C$_6$F$_5$ (**a**), 2,3,4,5-C$_6$F$_4$H (**b**), 2,3,5,6-C$_6$F$_4$H (**c**), 2,4,6-C$_6$F$_3$H$_2$ (**d**), 2,3-C$_6$F$_2$H$_3$ (**e**), 2,5-C$_6$F$_2$H$_3$ (**g**), and 2-C$_6$FH$_4$ (**h**), as stable crystalline compounds by the reactions of the [Tp′Rh(PR$_3$)] fragment with partially fluorinated benzene derivatives. The complexes were characterized by NMR spectroscopy and elemental analysis and the molecular structures were determined by X-ray crystallographic analysis. In the crystal structure, the Rh–Ar^F bond lengths were found to be strongly affected by the steric repulsion around the rhodium metal center rather than inductive effect of fluorine substituents. The kinetics of the reductive eliminations of fluoroarenes from the PMe$_3$ complexes (**3**) in benzene-d_6 solutions at 140 °C were investigated, but were unsuccessful because of the formation of Tp′Rh(PMe$_3$)$_2$ (**4**). Thermal reactions of the PMe$_2$Ph derivatives (**9**) in THF-d_8 solution at 120 °C, however, resulted in the intramolecular C–H bond activation of the phenyl group on the phosphine,

affording Tp′Rh(κ²-C_6H_4-2-PMe_2)H (**7**). The kinetics of the reductive eliminations of fluoroarenes from the complexes (**9**) were investigated and these results together with kinetic selectivities have shown the sensitivity of the Rh–Ar^F bond energies with *ortho*-fluorine substituents. The dependence of the Rh–Ar^F bond energy on the number of *ortho* fluorines is similar to that observed in the previously reported Tp′Rh(CNneopentyl)(Ar^F)H system. A plot of Rh–Ar^F *vs.* C–H bond strengths resulted in a line (slope = 2.15) that closely matches the DFT-calculated value (slope = 2.05), and is similar to that seen with Tp′Rh(CNneopentyl)(Ar^F)H system (slope = 2.14). This study also shows that the replacement of the isonitrile by a phosphine ligand does not increase the slope of the correlation. The experimental study gives the same slope for the phosphine and the isonitrile complexes while the DFT calculation finds only a small difference between the slopes. This difference is probably too small to be detectable in the experimental studies.

Experimental

General

All operations were performed under a nitrogen atmosphere unless otherwise stated, either on a high-vacuum line using modified Schlenk techniques or in a Vacuum Atmospheres Corp. Dri-Lab. Benzene-d_6, cyclohexane-d_{12} and THF-d_8 were distilled under vacuum from a dark purple solution of benzophenone ketyl and stored in an ampoule with a Teflon valve. Partially fluorinated aromatic compounds were purchased from Aldrich Chemical Co. and TCI America, dried over magnesium sulfate, and vacuum-distilled prior to use. Trimethylphosphine and dimethylphenylphosphine were purchased from Aldrich Chemical Co., dried over calcium hydride, and vacuum-distilled prior to use. Potassium tris(3,5-dimethylpyrazolyl)borate (KTp′) was purchased from TCI America, and purified by the previously reported recrystallization procedure[31] prior to use. The rhodium precursor *fac*-$RhCl_3(CH_3CN)_3$ was prepared according to the previously reported procedure.[32,33] The rhodium dihydride complexes Tp′$RhH_2(PMe_3)$ (**1**) and Tp′$RhH_2(PPhMe_2)$ (**5**) were prepared according to previously reported procedure, the latter employing PMe_2Ph in place of PMe_3.[25] Syntheses of Tp′Rh(C_6H_5)H(PMe_3) (**2**) and Tp′Rh(C_6D_5)D(PMe_3) (**2-d_6**) have been reported previously.[25] All ^{1}H, $^{13}C\{^1H\}$, $^{19}F\{^1H\}$ and $^{31}P\{^1H\}$ NMR spectra were recorded on a Bruker Avance 400 MHz NMR spectrometer. All ^{1}H chemical shifts are reported in ppm (δ) relative to tetramethylsilane and referenced to the chemical shift of residual solvent (benzene, δ 7.15). $^{13}C\{^1H\}$ NMR spectra were referenced to C_6D_6 (δ 128.0). $^{19}F\{^1H\}$ NMR spectra were referenced to external $C_6H_5CF_3$ (δ 0). $^{31}P\{^1H\}$ NMR spectra were referenced to external H_3PO_4 (δ 0). All temperatures for variable-temperature NMR spectroscopy were calibrated relative to the chemical shift differences in the NMR spectra of known standards (25–80 °C, ethylene glycol). All photolysis experiments were carried out using a water-filtered 200-W Hg–Xe lamp and filtered using a 270–370 nm band pass filter. Silica gel was heated overnight at 200 °C and then stored under nitrogen. A Bruker-AXS SMART platform diffractometer equipped with an APEX II CCD detector was used for X-ray crystal structure determination. Elemental analyses were obtained from Robertson Microlit Laboratories.

Preparation of Tp′Rh(Ar^F)H(PMe_3) (3) – general procedure

A resealable 5 mm NMR tube containing ~20 mg (0.042 mmol) of **1** was charged with 0.6 mL of Ar^FH in the glove box. The sample was irradiated, and the reaction was almost complete after 2 h of irradiation as determined by ^{1}H NMR spectroscopy. Powdered product was isolated in pure form by flash chromatography through silica gel in a glass fritted funnel using 5 : 1 hexane–THF as the eluent, removal of solvent, and then washing with ice-cold hexane.

For Tp′Rh(C_6F_5)H(PMe_3) (3a). Yield, 19.5 mg, 71%. Colorless plate crystals of **3a** suitable for X-ray crystallographic analysis were grown from 1 : 1 hexane : ether solution at room temperature. ^{1}H NMR (C_6D_6): δ −15.75 (dt, $^1J_{RhH} = {}^4J_{FH} = 19.4$ Hz, $^2J_{PH} = 24.8$ Hz, 1H, RhH), 0.99 (d, $^2J_{PH} = 9.6$ Hz, 9H, $P(CH_3)_3$), 1.52 (s, 3H, $pzCH_3$), 1.85 (s, 3H, $pzCH_3$), 2.03 (s, 3H, $pzCH_3$), 2.17 (s, 3H, $pzCH_3$), 2.18 (s, 3H, $pzCH_3$), 2.35 (s, 3H, $pzCH_3$), 5.38 (s, 1H, pzH), 5.57 (s, 1H, pzH), 5.82 (s, 1H, pzH). $^{13}C\{^1H\}$ NMR (C_6D_6): δ 12.77, 12.99, 13.08, 14.53, 16.08, 17.46 (s, $pzCH_3$), 19.90 (dd, $^1J_{PC} = 32.6$ Hz, $^2J_{RhC} = 1.8$ Hz, $P(CH_3)_3$), 106.03 (d, $^4J_{PC} = 2.5$ Hz, pzCH), 106.63 (s, pzCH), 106.83 (s, pzCH), 143.39 (d, $^3J_{PC} = 4.1$ Hz, pzCq), 143.59 (s, pzCq), 145.50 (s, pzCq), 149.56 (d, $^3J_{PC} = 3.5$ Hz, pzCq), 150.24 (s, pzCq), 150.66 (s, pzCq). Signals assignable to the six carbons of C_6F_5 group were not detected because of multiple coupling with fluorines. $^{19}F\{^1H\}$ NMR (C_6D_6): δ −41.81 (m, 1 F*ortho*), −55.81 (m, 1 F*ortho*), −100.52 (m, 1 F*para*), −102.15 (m, 1 F*meta*), −102.76 (m, 1 F*meta*). $^{31}P\{^1H\}$ NMR (C_6D_6): δ 0.82 (ddd, $^1J_{RhP} = 129.4$ Hz, $^4J_{FP} = 21.6$, 17.2 Hz, $RhP(CH_3)_3$). Anal. Calcd for $C_{24}H_{32}BF_5N_6PRh$: C, 44.74; H, 5.01. Found: C, 44.70; H, 4.73.

For Tp′Rh(2,3,4,5-C_6F_4H)H(PMe_3) (3b). Yield, 22.3 mg, 83%. Colorless plate crystals of **3b** suitable for X-ray crystallographic analysis were grown from hexane at −20 °C. ^{1}H NMR (C_6D_6): δ −16.22 (ddd, $^1J_{RhH} = 21.6$ Hz, $^2J_{PH} = 28.1$ Hz, $^4J_{FH} = 13.7$ Hz, 1H, RhH), 1.03 (d, $^2J_{PH} = 9.6$ Hz, 9H, $P(CH_3)_3$), 1.53 (s, 3H, $pzCH_3$), 1.84 (s, 3H, $pzCH_3$), 2.01 (s, 3H, $pzCH_3$), 2.14 (s, 3H, $pzCH_3$), 2.18 (s, 3H, $pzCH_3$), 2.33 (s, 3H, $pzCH_3$), 5.37 (s, 1H, pzH), 5.59 (s, 1H, pzH), 5.81 (s, 1H, pzH), 6.70 (m, 1H, Rh(*o*-C_6F_4H)). $^{13}C\{^1H\}$ NMR (C_6D_6): δ 12.69, 12.98, 13.08, 14.58, 16.23, 17.28 (s, $pzCH_3$), 20.12 (d, $^1J_{PC} = 32.6$ Hz, $P(CH_3)_3$), 106.40 (d, $^4J_{PC} = 3.3$ Hz, pzCH), 106.74 (s, pzCH), 107.44 (s, pzCH), 121.23 (m, CH, *o*-C_6F_4H), 143.35 (d, $^3J_{PC} = 2.6$ Hz, pzCq), 144.20 (s, pzCq), 145.17 (s, pzCq), 149.77 (s, pzCq), 150.26 (d, $^3J_{PC} = 2.2$ Hz, pzCq), 150.51 (s, pzCq). Signals assignable to the carbons of 2,3,5,6-C_6F_4H group except for the *ortho* carbon (CH) were not detected because of multiple coupling with fluorines. $^{19}F\{^1H\}$ NMR (C_6D_6): δ −47.90 (m, 1 F*ortho*), −81.29 (m, 1 F*para*), −97.68 (m, 1 F*meta*), −103.34 (m, 1 F*meta*). $^{31}P\{^1H\}$ NMR (C_6D_6): δ 1.24 (dm, $^1J_{RhP} = 131.2$ Hz). Anal. Calcd for $C_{24}H_{33}BF_4N_6PRh$: C, 46.03; H, 5.31; N, 13.42. Found: C, 46.30; H, 5.33; N, 13.21.

For Tp′Rh(2,3,5,6-C_6F_4H)H(PMe_3) (3c). Yield, 17.4 mg, 65%. ^{1}H NMR (C_6D_6): δ −15.66 (ddd, $^1J_{RhH} = 18.4$ Hz, $^2J_{PH} = 24.8$ Hz, $^4J_{FH} = 16.0$ Hz, 1H, RhH), 1.04 (d, $^2J_{PH} = 9.6$ Hz, 9H, $P(CH_3)_3$), 1.60 (s, 3H, $pzCH_3$), 1.92 (s, 3H, $pzCH_3$), 2.04 (s, 3H, $pzCH_3$), 2.20 (s×2, 3H×2, $pzCH_3$), 2.36 (s, 3H, $pzCH_3$), 5.39 (s, 1H, pzH), 5.58 (s, 1H, pzH), 5.83 (s, 1H, pzH), 6.52 (m, 1H, *p*-C_6F_4H). $^{13}C\{^1H\}$ NMR (C_6D_6): δ 12.78, 13.00, 13.07, 14.56, 16.11, 17.46 (s, $pzCH_3$), 20.00 (d, $^1J_{PC} = 32$ Hz, $P(CH_3)_3$), 100.36 (t, $^2J_{FC} = 23.5$ Hz, CH,

p-C_6F_4H), 106.01 (d, $^4J_{PC}$ = 3.6 Hz, pzCH), 106.60 (s, pzCH), 106.81 (s, pzCH), 143.28 (d, $^3J_{PC}$ = 2.5 Hz, pzCq), 143.50 (s, pzCq), 145.39 (s, pzCq), 149.62 (d, $^3J_{PC}$ = 2.5 Hz, pzCq), 150.26 (s, pzCq), 150.63 (s, pzCq). Signals assignable to the carbons of 2,3,5,6-C_6F_4H group except for the *para* carbon (CH) were not detected because of multiple coupling with fluorines. $^{19}F\{^1H\}$ NMR (C_6D_6): δ −57.21 (m, 1 F*ortho*), −59.83 (m, 1 F*ortho*), −79.00 (m, 1 F*meta*), −79.61 (m, 1 F*meta*). $^{31}P\{^1H\}$ NMR (C_6D_6): δ 0.96 (ddd, $^1J_{RhP}$ = 130.4 Hz, $^4J_{FP}$ = 22.5, 16.1 Hz). Anal. Calcd for $C_{24}H_{33}BF_4N_6PRh$: C, 46.03; H, 5.31; N, 13.42. Found: C, 46.04; H, 5.35; N, 13.17.

Tp′Rh(2,4,6-$C_6F_3H_2$)H(PMe_3) (3d). Yield, 23.7 mg, 91%. Colorless plate crystals of **3d** suitable for X-ray crystallographic analysis were grown from 1 : 1 hexane : ether solution at room temperature. ^1H NMR (C_6D_6): δ −15.88 (ddd, $^1J_{RhH}$ = 19.6 Hz, $^2J_{PH}$ = 25.8 Hz, $^4J_{FH}$ = 14.1 Hz, 1H, RhH), 1.10 (d, $^2J_{PH}$ = 9.6 Hz, 9H, $P(CH_3)_3$), 1.67 (s, 3H, $pzCH_3$), 2.00 (s, 3H, $pzCH_3$), 2.08 (s, 3H, $pzCH_3$), 2.21 (s, 3H, $pzCH_3$), 2.23 (s, 3H, $pzCH_3$), 2.37 (s, 3H, $pzCH_3$), 5.44 (s, 1H, pzH), 5.60 (s, 1H, pzH), 5.86 (s, 1H, pzH), 6.27 (m, 1H, $C_6F_3H_2$), 6.59 (m, 1H, $C_6F_3H_2$). $^{13}C\{^1H\}$ NMR (C_6D_6): δ 12.85, 13.05, 13.09, 14.63, 16.22, 17.46 (s, $pzCH_3$), 20.15 (d, $^1J_{PC}$ = 32.2 Hz, $P(CH_3)_3$), 97.48 (dd, $^2J_{FC}$ = 35.2, 23.8 Hz, CH, *m*-$C_6F_3H_2$), 98.71 (dd, $^2J_{FC}$ = 36.0, 22.7 Hz, CH, *m*-$C_6F_3H_2$), 105.90 (d, $^4J_{PC}$ = 3.3 Hz, pzCH), 106.44 (s, pzCH), 106.68 (s, pzCH), 143.05 (s, pzCq), 143.34 (s, pzCq), 145.11 (s, pzCq), 149.72 (s, pzCq), 150.18 (s, pzCq), 150.41 (s, pzCq). Signals for the carbons of 2,4,6-$C_6F_3H_2$ group except for the *meta* carbons (CH) could not be assigned because of multiple coupling with fluorines. $^{19}F\{^1H\}$ NMR (C_6D_6): δ −10.31 (m, 1 F*ortho*), −22.27 (m, 1 F*ortho*), −57.46 (m, 1 F*meta*). $^{31}P\{^1H\}$ NMR (C_6D_6): δ 1.36 (ddd, $^1J_{RhP}$ = 131.0 Hz, $^4J_{FP}$ = 20.1, 17.8 Hz). Anal. Calcd for $C_{24}H_{34}BF_3N_6PRh$: C, 47.39; H, 5.63; N, 13.82. Found: C, 47.28; H, 5.38; N, 13.64.

For Tp′Rh(2,3-$C_6F_2H_3$)H(PMe_3) (3e). **3e** forms along with its isomer, Tp′Rh(3,4-$C_6F_2H_3$)H(PMe_3), as judged by ^1H NMR spectroscopy. Heating at 120 °C for 2 weeks in 1,2-$C_6F_2H_4$ solution of the crude mixture resulted in the almost quantitative formation of **3e**. Yield, 21.3 mg, 84%. ^1H NMR (C_6D_6): δ −16.24 (ddd, $^1J_{RhH}$ = 22.2 Hz, $^2J_{PH}$ = 28.4 Hz, $^4J_{FH}$ = 13.2 Hz, 1H, RhH), 1.14 (d, $^2J_{PH}$ = 9.6 Hz, 9H, $P(CH_3)_3$), 1.60 (s, 3H, $pzCH_3$), 1.95 (s, 3H, $pzCH_3$), 2.08 (s, 3H, $pzCH_3$), 2.21 (s, 3H, $pzCH_3$), 2.22 (s, 3H, $pzCH_3$), 2.36 (s, 3H, $pzCH_3$), 5.40 (s, 1H, pzH), 5.63 (s, 1H, pzH), 5.86 (s, 1H, pzH), 6.38 (m, 1H, $C_6F_2H_3$), 6.70 (m, 1H, $C_6F_2H_3$), 6.86 (m, 1H, $C_6F_2H_3$). $^{13}C\{^1H\}$ NMR (C_6D_6): δ 12.72, 13.01, 13.12, 14.66, 16.48, 17.30 (s, $pzCH_3$), 20.37 (d, $^1J_{PC}$ = 32.4 Hz, $P(CH_3)_3$), 106.24 (d, $^4J_{PC}$ = 3.4 Hz, pzCH), 106.62 (s, pzCH), 107.19 (s, pzCH), 110.48 (d, $^2J_{FC}$ = 17.2 Hz, CH, *p*-$C_6F_2H_3$), 121.62 (d, $^3J_{FC}$ = 7.2 Hz, CH, *m*-$C_6F_2H_3$), 137.64 (d, $^3J_{FC}$ = 14.3 Hz, CH, *o*-$C_6F_2H_3$), 142.32 (m, br, C, *ipso*-$C_6F_2H_3$), 142.98 (d, $^3J_{PC}$ = 2.2 Hz, pzCq), 143.82 (s, pzCq) 144.87 (s, pzCq), 149.87 (s, pzCq), 150.02 (dd, $^1J_{FC}$ = 246.7 Hz, $^2J_{FC}$ = 32.2 Hz, CF, *m*-$C_6F_2H_3$), 150.39 (s, pzCq), 150.54 (d, $^3J_{PC}$ = 2.3 Hz, pzCq), 156.15 (dm, $^1J_{FC}$ = 226.6 Hz, CF, *o*-$C_6F_2H_3$). $^{19}F\{^1H\}$ NMR (C_6D_6): δ −47.15 (m, 1 F*ortho*), −78.43 (m, 1 F*meta*). $^{31}P\{^1H\}$ NMR (C_6D_6): δ 1.69 (dm, $^1J_{RhP}$ = 131.3 Hz). Anal. Calcd for $C_{24}H_{35}BF_2N_6PRh$: C, 48.84; H, 5.98; N, 14.24. Found: C, 49.11; H, 6.03; N, 14.37.

For Tp′Rh(2,6-$C_6F_2H_3$)H(PMe_3) (3f). **3f** forms along with the isomers, Tp′Rh(2,4-$C_6F_2H_3$)H(PMe_3) and Tp′Rh(3,5-$C_6F_2H_3$)H(PMe_3), as judged by ^1H NMR spectroscopy. Heating at 120 °C for 1 month or more of 1,3-$C_6F_2H_4$ solution of the crude mixture did not result in the quantitative formation of **3f** and **3f** could not be isolated as pure form. For **3f** (major product): ^1H NMR (C_6D_6): δ −16.24 (ddd, $^1J_{RhH}$ = 22.2 Hz, $^2J_{PH}$ = 28.9 Hz, $^4J_{FH}$ = 12.0 Hz, 1H, RhH), 1.12 (d, $^2J_{PH}$ = 9.6 Hz, 9H, $P(CH_3)_3$), 1.61 (s, 3H, $pzCH_3$), 1.93 (s, 3H, $pzCH_3$), 2.09 (s, 3H, $pzCH_3$), 2.21 (s, 3H, $pzCH_3$), 2.22 (s, 3H, $pzCH_3$), 2.36 (s, 3H, $pzCH_3$), 5.43 (s, 1H, pzH), 5.63 (s, 1H, pzH), 5.86 (s, 1H, pzH), 6.39 (m, 1H, $C_6F_2H_3$), 6.73 (m, 1H, $C_6F_2H_3$), 6.96 (m, 1H, $C_6F_2H_3$). $^{19}F\{^1H\}$ NMR (C_6D_6): δ −18.67 (m, 1 F*ortho*), −25.49 (m, 1 F*ortho*). $^{31}P\{^1H\}$ NMR (C_6D_6): δ 1.94 (dm, $^1J_{RhP}$ = 130.7 Hz, $RhP(CH_3)_3$).

For Tp′Rh(2,5-$C_6F_2H_3$)H(PMe_3) (3g). Yield, 22.5 mg, 89%. Colorless plate crystals of **3g** suitable for X-ray crystallographic analysis were grown from 1 : 1 hexane : ether solution at room temperature. ^1H NMR (C_6D_6): δ −16.23 (ddd, $^1J_{RhH}$ = 22.2 Hz, $^2J_{PH}$ = 28.3 Hz, $^4J_{FH}$ = 11.9 Hz, 1H, RhH), 1.16 (d, $^2J_{PH}$ = 9.6 Hz, 9H, $P(CH_3)_3$), 1.67 (s, 3H, $pzCH_3$), 1.98 (s, 3H, $pzCH_3$), 2.04 (s, 3H, $pzCH_3$), 2.21 (s×2, 3H×2, $pzCH_3$), 2.36 (s, 3H, $pzCH_3$), 5.40 (s, 1H, pzH), 5.62 (s, 1H, pzH), 5.82 (s, 1H, pzH), 6.56 (m, 1H, $C_6F_2H_3$), 6.71 (m, 1H, $C_6F_2H_3$), 6.97 (m, 1H, $C_6F_2H_3$). $^{13}C\{^1H\}$ NMR (C_6D_6): δ 12.74, 13.04, 13.10, 14.70, 16.32, 17.29 (s, $pzCH_3$), 20.29 (d, $^1J_{PC}$ = 32.3 Hz, $P(CH_3)_3$), 106.34 (d, $^4J_{PC}$ = 3.4 Hz, pzCH), 106.59 (s, pzCH), 107.33 (s, pzCH), 109.59 (dd, $^2J_{FC}$ = 24.6 Hz, $^3J_{FC}$ = 9.3 Hz, CH, *m*-$C_6F_2H_3$), 112.47 (dd, $^2J_{FC}$ = 35.8 Hz, $^3J_{FC}$ = 8.5 Hz, CH, *p*-$C_6F_2H_3$), 142.24 (m, br, C, *ipso*-$C_6F_2H_3$), 143.10 (d, $^3J_{PC}$ = 2.4 Hz, pzCq), 143.98 (s, pzCq), 144.85 (s, pzCq), 149.77 (s, pzCq), 150.27 (s, pzCq), 150.43 (d, $^3J_{PC}$ = 2.4 Hz, pzCq), 157.89 (d, $^1J_{FC}$ = 241.5 Hz, CF, *m*-$C_6F_2H_3$), 165.34 (d, $^1J_{FC}$ = 223.7 Hz, CF, *o*-$C_6F_2H_3$). The signal assignable to the *ortho* CH of 2,5-$C_6F_2H_3$ group was not detected because of overlap with solvent peaks. $^{19}F\{^1H\}$ NMR (C_6D_6): δ −28.35 (m, 1 F*ortho*), −60.54 (m, 1 F*meta*). $^{31}P\{^1H\}$ NMR (C_6D_6): δ 1.69 (dm, $^1J_{RhP}$ = 132.7 Hz). Anal. Calcd for $C_{24}H_{35}BF_2N_6PRh$: C, 48.84; H, 5.98; N, 14.24. Found: C, 48.61; H, 5.81; N, 14.07.

For Tp′Rh(2-C_6FH_4)H(PMe_3) (3h). Yield, 17.2 mg, 70%. ^1H NMR (C_6D_6): δ −16.32 (ddd, $^1J_{RhH}$ = 22.8 Hz, $^2J_{PH}$ = 28.4 Hz, $^4J_{FH}$ = 12.0 Hz, 1H, RhH), 1.24 (d, $^2J_{PH}$ = 9.6 Hz, 9H, $P(CH_3)_3$), 1.73 (s, 3H, $pzCH_3$), 2.00 (s, 3H, $pzCH_3$), 2.10 (s, 3H, $pzCH_3$), 2.25 (s, 3H, $pzCH_3$), 2.27 (s, 3H, $pzCH_3$), 2.45 (s, 3H, $pzCH_3$), 5.43 (s, 1H, pzH), 5.64 (s, 1H, pzH), 5.87 (s, 1H, pzH), 6.59 (m, 1H, C_6FH_4), 6.61 (m, 1H, C_6FH_4), 6.86 (m, 1H, C_6FH_4), 6.92 (m, 1H, C_6FH_4). $^{13}C\{^1H\}$ NMR (C_6D_6): δ 12.76, 13.05, 13.14, 14.70, 16.50, 17.30 (s, $pzCH_3$), 20.48 (d, $^1J_{PC}$ = 32.2 Hz, $P(CH_3)_3$), 106.21 (d, $^4J_{PC}$ = 3.4 Hz, pzCH), 106.52 (s, pzCH), 107.15 (s, pzCH), 125.59 (d, $^2J_{FC}$ = 31.6 Hz, CH, *m*-C_6FH_4), 122.23 (s, CH, *m*-C_6FH_4), 123.62 (d, $^3J_{FC}$ = 8.0 Hz, CH, *p*-C_6FH_4), 138.15 (ddd, $^1J_{RhC}$ = 40.4 Hz, $^2J_{PC}$ = 15.9 Hz, $^2J_{FC}$ = 32.5 Hz, C, *ipso*-C_6FH_4), 124.83 (s, pzCq), 143.40 (d, $^3J_{FC}$ = 15.5 Hz, CH, *o*-C_6FH_4), 143.73 (s, pzCq), 144.67 (s, pzCq), 149.86 (s, pzCq), 150.20 (s, pzCq) 150.65 (s, pzCq), 169.33 (d, $^1J_{FC}$ = 231.5 Hz, CF, *o*-C_6FH_4). $^{19}F\{^1H\}$ NMR (C_6D_6): δ −20.41 (m, 1 F*ortho*). $^{31}P\{^1H\}$ NMR (C_6D_6): δ 2.03 (dm, $^1J_{RhP}$ = 131.4 Hz). Anal. Calcd for $C_{24}H_{36}BFN_6PRh$: C, 50.37; H, 6.34; N, 14.69. Found: C, 50.20; H, 6.10; N, 14.48.

Preparation of Tp′Rh(C_6H_5)H($PPhMe_2$) (6)

A resealable 5 mm NMR tube containing 20.5 mg (0.0380 mmol) of **5** was charged with 0.7 mL of C_6H_6 in the glove box. The

sample was irradiated, and after 5 h the starting material **5** had disappeared completely as judged by the ^{1}H NMR spectroscopy. **6** and **7** were seen in a ratio of 6.8 : 1. Heating at 120 °C for 1 h in C_6H_6 solution resulted in the almost quantitative formation of **6**. **6** was isolated as a colorless powder (16.4 mg, 0.0266 mmol, 70%) in pure form by flash chromatography through silica gel in a glass frit funnel using 5 : 1 hexane–THF as the eluent, removal of solvent, and then washing with a minimum amount of ice-cold hexane three times. ^{1}H NMR (C_6D_6): δ –16.29 (dd, $^1J_{RhH}$ = 23.3 Hz, $^2J_{PH}$ = 27.6 Hz, 1H, RhH), 1.29 (d, $^2J_{PH}$ = 8.8 Hz, 3H, PPhMe_2), 1.63 (s, 3H, pzCH$_3$), 1.72 (d, $^2J_{PH}$ = 8.4 Hz, 3H, PPhMe_2), 1.85 (s, 3H, pzCH$_3$), 2.02 (s, 3H, pzCH$_3$), 2.15 (s, 3H, pzCH$_3$), 2.25 (s, 3H, pzCH$_3$), 2.42 (s, 3H, pzCH$_3$), 5.45 (s, 1H, pzH), 5.52 (s, 1H, pzH), 5.89 (s, 1H, pzH), 6.84 (t, J = 7.4 Hz, 1H, RhPh), 6.93 (m, 3H, PPhMe$_2$), 7.00 (t, J = 7.0 Hz, 1H, RhPh), 7.13 (t, J = 7.0 Hz, 1H, RhPh), 7.26 (d, J = 7.6 Hz, 1H, RhPh), 7.66 (m, 2H, PPhMe$_2$), 7.91 (d, J = 6.8 Hz, 1H, RhPh). ^{13}C{^{1}H} NMR (C_6D_6): δ 12.86, 13.12, 13.20, 15.50, 16.02, 16.78 (s, pzCH$_3$), 18.36 (d, $^1J_{PC}$ = 29.8 Hz, PPhMe_2), 21.94 (dd, $^1J_{PC}$ = 35.0 Hz, $^2J_{RhC}$ = 2.4 Hz, PPhMe_2), 106.29 (s, pzCH), 106.40 (d, $^4J_{PC}$ = 4.0 Hz, pzCH), 107.23 (s, pzCH), 121.70 (s, RhPh), 125.91 (s, RhPh), 126.26 (s, RhPh), 129.70 (s, PPhMe$_2$), 131.36 (d, $^1J_{PC}$ = 10.7 Hz, PPhMe$_2$), 138.38 (s, PPhMe$_2$), 138.80 (s, PPhMe$_2$), 141.08 (s, RhPh), 142.80 (d, $^3J_{PC}$ = 2.0 Hz, pzCq), 143.86 (s, pzCq), 145.01 (s, RhPh), 144.98 (d, $^3J_{PC}$ = 6.1 Hz, pzCq), 150.23 (s, pzCq), 150.40 (s, pzCq), 151.17 (s, pzCq), 154.22 (dd, $^1J_{RhC}$ = 35.2 Hz, $^2J_{PC}$ = 13.1 Hz, *ipso*- RhPh). ^{31}P{^{1}H} NMR (C_6D_6): δ 15.35 (d, $^1J_{RhP}$ = 149.5 Hz). Anal. Calcd for $C_{29}H_{39}BN_6PRh$: C, 56.51; H, 6.38; N, 13.64. Found: C, 56.28; H, 6.25; N, 13.40.

Preparation of Tp′Rh(C_6D_5)D(PPhMe$_2$) (6-d_6)

Prepared as for **6** but with C_6D_6 solvent. Anal. Calcd for $C_{29}H_{33}D_6BN_6PRh$: C, 55.96; H, 6.23; N, 13.50. Found: C, 55.68; H, 6.33; N, 13.30.

Preparation of Tp′Rh(κ^2-C_6H_4-2-PMe$_2$)H (7)

A resealable 5 mm NMR tube containing 16.4 mg (0.0266 mmol) of **6** was charged with 0.7 mL of THF in the glove box. Heating of the sample at 120 °C for 1 h resulted in the almost quantitative formation of **7**. **7** was obtained as a colorless powder (12.0 mg, 0.0223 mmol, 84%) in pure form by washing with ice-cold hexane. Colorless single crystals of **7** suitable for X-ray crystallographic analysis were grown from hexane at –20 °C. **7**: ^{1}H NMR (C_6D_6): δ –14.93 (dd, $^1J_{RhH}$ = 22.0 Hz, $^2J_{PH}$ = 35.2 Hz, 1H, RhH), 1.12 (d, $^2J_{PH}$ = 10.8 Hz, 3H, η^2-C_6H_4–PMe_2), 1.50 (s, 3H, pzCH$_3$), 1.58 (d, $^2J_{PH}$ = 10.4 Hz, 3H, η^2-C_6H_4–PMe_2), 2.16 (s, 3H, pzCH$_3$), 2.25 (s×2, 3H×2, pzCH$_3$), 2.26 (s, 3H, pzCH$_3$), 2.52 (s, 3H, pzCH$_3$), 5.63 (s, 1H, pzH), 5.71 (s×2, 1H×2, pzH), 6.69 (m, 1H, η^2-C_6H_4-PMe$_2$), 6.95 (m, 1H, η^2-C_6H_4-PMe$_2$), 7.02 (t, J = 7.4 Hz, 1H, η^2-C_6H_4-PMe$_2$), 7.34 (t, J = 5.6 Hz, 1H, η^2-C_6H_4-PMe$_2$). ^{13}C{^{1}H} NMR (C_6D_6): δ 12.32 (d, $^1J_{PC}$ = 13.4 Hz, η^2-C_6H_4–PMe_2), 12.71, 12.83, 12.93 (s×2), 16.01, 16.18 (s, pzCH$_3$), 20.53 (d, $^1J_{PC}$ = 33.1 Hz, η^2-C_6H_4–PMe_2), 105.48 (s, pzCH), 106.01 (d, $^4J_{PC}$ = 4.9 Hz, pzCH), 107.23 (s, pzCH), 122.39 (d, J = 9.8 Hz, η^2-C_6H_4-PMe$_2$), 123.32 (s, η^2-C_6H_4-PMe$_2$), 129.75 (s, η^2-C_6H_4-PMe$_2$), 135.57 (d, J = 10.3 Hz, η^2-C_6H_4-PMe$_2$), 143.24 (s, pzCq), 143.38 (s, pzCq), 143.45 (d, $^3J_{PC}$ = 2.2 Hz, pzCq), 148.86 (s, pzCq), 150.30 (s, pzCq), 150.76 (s, pzCq), 151.75 (s, η^2-C_6H_4-PMe$_2$), 151.95 (d, $^1J_{RhC}$ = 31.7 Hz, *ipso*-η^2-C_6H_4-PMe$_2$). ^{31}P{^{1}H} NMR (C_6D_6): δ –65.12 (d, $^1J_{RhP}$ = 114.2 Hz). Anal. Calcd for $C_{23}H_{33}BN_6PRh$: C, 51.32; H, 6.18; N, 15.61. Found: C, 51.51; H, 5.97; N, 15.38.

Preparation of Tp′Rh(Ar^F)H(PPhMe$_2$) (9) – general procedure

A resealable 5 mm NMR tube containing ~20 mg (0.038 mmol) of **5** was charged with 0.7 mL of Ar^{F}H in the glove box. The sample was irradiated for 5 h, at which point the starting material **5** had disappeared completely as judged by the ^{1}H NMR spectroscopy to form **9** and **7** (ratio given in Schemes 6 and 7). Heating the mixture at 120 °C for 1 h in Ar^{F}H solution resulted in the almost quantitative formation of **9**. The product was obtained as a powder by flash chromatography through silica gel in a glass fritted funnel using 5 : 1 hexane–THF as the eluent, removal of solvent, and then washing with a minimum amount of ice-cold hexane.

For Tp′Rh(C_6F_5)H(PPhMe$_2$) (9a). Yield, 22.1 mg, 0.0312 mmol, 82%. Colorless single crystals of **9a** suitable for X-ray crystallographic analysis were grown from hexane at –20 °C. **9a**: ^{1}H NMR (C_6D_6): δ –15.18 (dt, $^1J_{RhH}$ = $^4J_{FH}$ = 16.0 Hz, $^2J_{PH}$ = 23.6 Hz, 1H, RhH), 1.17 (d, $^2J_{PH}$ = 6.0 Hz, 3H, PPhMe_2), 1.53 (d, $^2J_{PH}$ = 9.2 Hz, 3H, PPhMe_2), 1.56 (s, 3H, pzCH$_3$), 1.61 (s, 3H, pzCH$_3$), 1.79 (s, 3H, pzCH$_3$), 2.06 (s, 3H, pzCH$_3$), 2.18 (s, 3H, pzCH$_3$), 2.38 (s, 3H, pzCH$_3$), 5.33 (s, 1H, pzH), 5.41 (s, 1H, pzH), 5.82 (s, 1H, pzH), 6.95 (m, 3H, PPhMe$_2$), 7.61 (m, 2H, PPhMe$_2$). ^{13}C{^{1}H} NMR (C_6D_6): δ 12.77, 12.97, 13.14, 14.70, 15.94, 16.21 (s, pzCH$_3$), 17.24 (d, $^1J_{PC}$ = 30.4 Hz, PPhMe_2), 22.20 (dd, $^1J_{PC}$ = 33.4 Hz, $^2J_{RhC}$ = 3.4 Hz, PPhMe_2), 106.19 (d, $^4J_{PC}$ = 3.1 Hz, pzCH), 106.74 (s, pzCH), 107.00 (s, pzCH), 129.90 (s, PPhMe$_2$), 131.61 (dd, $^1J_{PC}$ = 9.8 Hz, $^2J_{RhC}$ = 4.0 Hz, PPhMe$_2$), 138.05 (s, PPhMe$_2$), 138.50 (s, PPhMe$_2$), 143.45 (d, $^3J_{PC}$ = 2.2 Hz, pzCq), 143.57 (s, pzCq), 145.24 (s, pzCq), 149.75 (s, pzCq), 150.42 (s, pzCq), 151.68 (s, pzCq). Signals assignable to the six carbons of C_6F_5 group were not detected because of multiple coupling with fluorines. ^{19}F{^{1}H} NMR (C_6D_6): δ –40.56 (m, 1 F*ortho*), –55.38 (m, 1 F*ortho*), –100.14 (m, 1 F*para*), –101.98 (m, 1 F*meta*), –102.62 (m, 1 F*meta*). ^{31}P{^{1}H} NMR (C_6D_6): δ 10.23 (ddd, $^1J_{RhP}$ = 132.4 Hz, $^4J_{FP}$ = 13.4, 8.2 Hz). Anal. Calcd for $C_{29}H_{34}BF_5N_6PRh$: C, 49.31; H, 4.85; N, 11.90. Found: C, 49.57; H, 4.77; N, 11.67.

For Tp′Rh(2,3,4,5-C_6F_4H)H(PPhMe$_2$) (9b). Yield, 20.5 mg, 79%. Colorless single crystals of **9b** suitable for X-ray crystallographic analysis were grown from hexane at –20 °C. ^{1}H NMR (C_6D_6): δ –15.59 (ddd, $^1J_{RhH}$ = 19.6 Hz, $^2J_{PH}$ = 26.6 Hz, $^4J_{FH}$ = 12.8 Hz, 1H, RhH), 1.25 (d, $^2J_{PH}$ = 9.2 Hz, 3H, PPhMe_2), 1.67 (s, 3H, pzCH$_3$), 1.74 (d, $^2J_{PH}$ = 4.2 Hz, 3H, PPhMe_2), 1.75 (s, 3H, pzCH$_3$), 1.86 (s, 3H, pzCH$_3$), 2.12 (s, 3H, pzCH$_3$), 2.26 (s, 3H, pzCH$_3$), 2.41 (s, 3H, pzCH$_3$), 5.47 (s, 1H, pzH), 5.49 (s, 1H, pzH), 5.90 (s, 1H, pzH), 6.80 (m, 1H, Rh(*o*-C_6F_4H)), 7.01 (m, 3H, PPhMe$_2$), 7.65 (m, 2H, PPhMe$_2$). ^{13}C{^{1}H} NMR (C_6D_6): δ 12.71, 13.00, 13.16, 14.79, 16.14, 16.21 (s, pzCH$_3$), 17.97 (d, $^1J_{PC}$ = 30.6 Hz, PPhMe_2), 22.82 (dm, $^1J_{PC}$ = 39.3 Hz, PPhMe_2), 106.54 (d, $^4J_{PC}$ = 4.1 Hz, pzCH), 106.81 (s, pzCH), 107.61 (s, pzCH), 121.32 (m, CH, *o*-C_6F_4H), 129.92 (s, PPhMe$_2$), 131.55 (dd, $^1J_{PC}$ = 10.7 Hz, $^2J_{RhC}$ = 3.0 Hz, PPhMe$_2$), 137.72 (s, PPhMe$_2$), 138.16 (s, PPhMe$_2$), 143.46 (s, pzCq), 144.28 (s, pzCq), 144.82 (s, pzCq), 150.09 (s, pzCq), 150.53 (s, pzCq), 151.40 (s, pzCq). Signals assignable to the six carbons of 2,3,4,5-C_6F_4H group except for the

ortho carbon (CH) were not detected because of multiple coupling with fluorines. $^{19}F\{^1H\}$ NMR (C_6D_6): δ –47.05 (m, 1 F*ortho*), –81.12 (m, 1 F*para*), –97.47 (m, 1 F*meta*), –102.91 (m, 1 F*meta*). $^{31}P\{^1H\}$ NMR (C_6D_6): δ 11.12 (dm, $^1J_{RhP}$ = 136.8 Hz). Anal. Calcd for $C_{29}H_{35}BF_4N_6PRh$: C, 50.60; H, 5.13; N, 12.21. Found: C, 50.34; H, 4.89; N, 11.97.

For Tp′Rh(2,3,5,6-C_6F_4H)H(PPhMe_2) (9c). Yield, 19.9 mg, 76%. Colorless single crystals of **9c** suitable for X-ray crystallographic analysis were grown from hexane at –20 °C. **9c**: ^1H NMR (C_6D_6): δ –15.09 (dt, $^1J_{RhH} = {}^4J_{FH}$ = 15.2 Hz, $^2J_{PH}$ = 23.6 Hz, 1H, RhH), 1.21 (d, $^2J_{PH}$ = 9.2 Hz, 3H, PPh*Me*$_2$), 1.59 (s, 3H, pzCH_3), 1.60 (d, $^2J_{PH}$ = 8.0 Hz, 3H, PPh*Me*$_2$), 1.68 (s, 3H, pzCH_3), 1.85 (s, 3H, pzCH_3), 2.07 (s, 3H, pzCH_3), 2.19 (s, 3H, pzCH_3), 2.39 (s, 3H, pzCH_3), 5.39 (s, 1H, pzH), 5.42 (s, 1H, pzH), 5.82 (s, 1H, pzH), 6.53 (m, 1H, Rh(*p*-C_6F_4H)), 6.95 (m, 3H, P*Ph*Me$_2$), 7.66 (m, 2H, P*Ph*Me$_2$). $^{13}C\{^1H\}$ NMR (C_6D_6): δ 12.78, 12.99, 13.13, 14.74, 19.92, 16.24 (s, pzCH_3), 17.41 (d, $^1J_{PC}$ = 30.3 Hz, PPh*Me*$_2$), 22.37 (d, $^1J_{PC}$ = 29.6 Hz, PPh*Me*$_2$), 100.59 (t, $^2J_{FC}$ = 23.3 Hz, CH, *p*-C_6F_4H), 106.18 (d, $^4J_{PC}$ = 3.4 Hz, pzCH), 106.71 (s, pzCH), 106.94 (s, pzCH), 129.80 (s, P*Ph*Me$_2$), 131.70 (dd, $^1J_{PC}$ = 9.8 Hz, $^2J_{RhC}$ = 4.4 Hz, P*Ph*Me$_2$), 138.24 (s, P*Ph*Me$_2$), 138.69 (s, P*Ph*Me$_2$), 143.41 (d, $^3J_{PC}$ = 2.2 Hz, pzCq), 143.48 (s, pzCq), 145.13 (s, pzCq), 149.81 (s, pzCq), 150.45 (s, pzCq), 151.64 (s, pzCq). Signals assignable to the carbons of 2,3,5,6-C_6F_4H group except for the *para* carbon (CH) were not detected because of multiple coupling with fluorines. $^{19}F\{^1H\}$ NMR (C_6D_6): δ –41.67 (m, 1 F*ortho*), –57.03 (m, 1 F*ortho*), –79.16 (m, 1 F*meta*), –80.01 (m, 1 F*meta*). $^{31}P\{^1H\}$ NMR (C_6D_6): δ 10.40 (dm, $^1J_{RhP}$ = 133.0 Hz). Anal. Calcd for $C_{29}H_{35}BF_4N_6PRh$: C, 50.60; H, 5.13; N, 12.21. Found: C, 50.82; H, 4.88; N, 11.95.

For Tp′Rh(2,4,6-$C_6F_3H_2$)H(PPhMe_2) (9d). Yield, 21.6 mg, 85%. Colorless crystals of **9d** suitable for X-ray crystallographic analysis were grown from hexane at –20 °C. ^1H NMR (C_6D_6): δ –15.33 (ddd, $^1J_{RhH}$ = 17.6 Hz, $^2J_{PH}$ = 24.0 Hz, $^4J_{FH}$ = 14.0 Hz, 1H, RhH), 1.28 (d, $^2J_{PH}$ = 8.8 Hz, 3H, PPh*Me*$_2$), 1.63 (s, 3H, pzCH_3), 1.67 (d, $^2J_{PH}$ = 8.8 Hz, 3H, PPh*Me*$_2$), 1.75 (s, 3H, pzCH_3), 1.92 (s, 3H, pzCH_3), 2.11 (s, 3H, pzCH_3), 2.21 (s, 3H, pzCH_3), 2.41 (s, 3H, pzCH_3), 5.42 (s, 1H, pzH), 5.48 (s, 1H, pzH), 5.86 (s, 1H, pzH), 6.26 (m, 1H, Rh(*m*-C_6F_4H)), 6.61 (m, 1H, Rh(*m*-C_6F_4H)), 6.97 (m, 3H, P*Ph*Me$_2$), 7.71 (m, 2H, P*Ph*Me$_2$). $^{13}C\{^1H\}$ NMR (C_6D_6): δ 12.85, 13.05, 13.17, 14.82, 16.08, 16.34 (s, pzCH_3), 17.68 (d, $^1J_{PC}$ = 30.0 Hz, PPh*Me*$_2$), 22.63 (d, $^1J_{PC}$ = 28.9 Hz, PPh*Me*$_2$), 97.53 (dd, $^2J_{FC}$ = 36.6, 19.4 Hz, CH, *m*-$C_6F_3H_2$), 98.84 (dd, $^2J_{FC}$ = 35.9, 23.0 Hz, CH, *m*-$C_6F_3H_2$), 106.10 (d, $^4J_{PC}$ = 3.5 Hz, pzCH), 106.56 (s, pzCH), 106.82 (s, pzCH), 129.73 (s, P*Ph*Me$_2$), 131.85 (dd, $^1J_{PC}$ = 9.9 Hz, $^2J_{RhC}$ = 4.2 Hz, P*Ph*Me$_2$), 138.58 (s, P*Ph*Me$_2$), 139.02 (s, P*Ph*Me$_2$), 143.11 (d, $^3J_{PC}$ = 2.6 Hz, pzCq), 143.29 (s, pzCq), 144.83 (s, pzCq), 149.96 (s, pzCq), 150.39 (s, pzCq), 151.38 (s, pzCq). Signals for the carbons of 2,4,6-$C_6F_3H_2$ group except for the *meta* carbons (CH) could not be assigned because of multiple coupling with fluorines. $^{19}F\{^1H\}$ NMR (C_6D_6): δ –8.66 (m, 1 F*ortho*), –21.52 (m, 1 F*ortho*), –57.21 (m, 1 F*para*). $^{31}P\{^1H\}$ NMR (C_6D_6): δ 11.07 (dm, $^1J_{RhP}$ = 133.5 Hz). Anal. Calcd for $C_{29}H_{36}BF_3N_6PRh$: C, 51.96; H, 5.41; N, 12.54. Found: C, 51.69; H, 5.33; N, 12.34.

Tp′Rh(2,3-$C_6F_2H_3$)H(PPhMe_2) (9e). Photolysis resulted in the formation of **9e** with the isomer Tp′Rh(3,4-$C_6F_2H_3$)H(PPhMe_2), and **7**, as judged by ^1H NMR spectroscopy. Heating at 120 °C for 1 h in 1,2-$C_6F_2H_4$ solution resulted in the quantitative formation of **9e**. Yield, 21.9 mg, 89%. Colorless single crystals of **9e** suitable for X-ray crystallographic analysis were grown from hexane at –20 °C. **9e**: ^1H NMR (C_6D_6): δ –15.70 (ddd, $^1J_{RhH}$ = 20.2 Hz, $^2J_{PH}$ = 27.0 Hz, $^4J_{FH}$ = 12.0 Hz, 1H, RhH), 1.28 (d, $^2J_{PH}$ = 9.2 Hz, 3H, PPh*Me*$_2$), 1.65 (s, 3H, pzCH_3), 1.72 (s, 3H, pzCH_3), 1.80 (d, $^2J_{PH}$ = 9.2 Hz, 3H, PPh*Me*$_2$), 1.87 (s, 3H, pzCH_3), 2.11 (s, 3H, pzCH_3), 2.22 (s, 3H, pzCH_3), 2.39 (s, 3H, pzCH_3), 5.43 (s, 1H, pzH), 5.44 (s, 1H, pzH), 5.84 (s, 1H, pzH), 6.37 (m, 1H, $C_6F_2H_3$), 6.71 (m, 1H, $C_6F_2H_3$), 6.88 (m, 1H, $C_6F_2H_3$), 6.92 (m, 3H, P*Ph*Me$_2$), 7.63 (m, 2H, P*Ph*Me$_2$). $^{13}C\{^1H\}$ NMR (C_6D_6): δ 12.74, 13.04, 13.22, 14.88, 16.28, 16.36 (s, pzCH_3), 18.33 (d, $^1J_{PC}$ = 30.5 Hz, PPh*Me*$_2$), 23.26 (dd, $^1J_{PC}$ = 35.3 Hz, $^2J_{RhC}$ = 2.9 Hz, PPh*Me*$_2$), 106.37 (d, $^4J_{PC}$ = 3.3 Hz, pzCH), 106.63 (s, pzCH), 107.36 (s, pzCH), 110.68 (d, $^2J_{FC}$ = 17.1 Hz, CH, *p*-$C_6F_2H_3$), 121.61 (d, $^3J_{FC}$ = 4.4 Hz, CH, *m*-$C_6F_2H_3$), 129.75 (s, P*Ph*Me$_2$), 131.74 (dd, $^1J_{PC}$ = 10.2 Hz, $^2J_{RhC}$ = 2.2 Hz, P*Ph*Me$_2$), 137.65 (d, $^3J_{FC}$ = 14.1 Hz, CH, *o*-$C_6F_2H_3$), 138.13 (s, P*Ph*Me$_2$), 138.56 (s, P*Ph*Me$_2$), 141.62 (dddd, br, $^1J_{RhC}$ = 41.2 Hz, C, *ipso*-$C_6F_2H_3$), 143.04 (d, $^3J_{PC}$ = 2.5 Hz, pzCq), 143.87 (s, pzCq), 144.51 (s, pzCq), 150.10 (dd, $^1J_{FC}$ = 245.2 Hz, $^2J_{FC}$ = 22.6 Hz, CF, *m*-$C_6F_2H_3$). 150.20 (s, pzCq), 150.82 (s, pzCq), 151.46 (s, pzCq), 156.48 (dm, $^1J_{FC}$ = 225.0 Hz, CF, *o*-$C_6F_2H_3$). $^{19}F\{^1H\}$ NMR (C_6D_6): δ –46.30 (m, 1 F*ortho*), –78.25 (m, 1 F*meta*). $^{31}P\{^1H\}$ NMR (C_6D_6): δ 11.60 (ddd, $^1J_{RhP}$ = 140.1 Hz, $^4J_{FP}$ = 16.7, 6.5 Hz). Anal. Calcd for $C_{29}H_{37}BF_2N_6PRh$: C, 53.39; H, 5.72; N, 12.88. Found: C, 53.21; H, 5.51; N, 12.85.

For Tp′Rh(2,6-$C_6F_2H_3$)H(PPhMe_2) (9f). Photolysis resulted in the formation of **9f** with the isomers Tp′Rh(2,4-$C_6F_2H_3$)H(PPhMe_2) and Tp′Rh(3,5-$C_6F_2H_3$)H(PPhMe_2), and **7**, as judged by ^1H NMR spectroscopy. Heating at 120 °C for more than 1 month in 1,3-$C_6F_2H_4$ solution the crude mixture did not afford the pure **9f** and it could not be isolated as pure form. For **9f**: ^1H NMR (C_6D_6): δ –15.83 (ddd, $^1J_{RhH}$ = 20.2 Hz, $^2J_{PH}$ = 27.6 Hz, $^4J_{FH}$ = 11.2 Hz, 1H, RhH), 1.24 (d, $^2J_{PH}$ = 8.9 Hz, 3H, PPh*Me*$_2$), 1.72 (s, 3H, pzCH_3), 1.81 (s, 3H, pzCH_3), 1.88 (d, $^2J_{PH}$ = 8.9 Hz, 3H, PPh*Me*$_2$), 1.91 (s, 3H, pzCH_3), 2.09 (s, 3H, pzCH_3), 2.18 (s, 3H, pzCH_3), 2.40 (s, 3H, pzCH_3), 5.44 (s, 1H, pzH), 5.47 (s, 1H, pzH), 5.86 (s, 1H, pzH), 6.37 (m, 1H, Rh(*m*-$C_6F_2H_3$)), 6.77 (m, 1H, Rh(*m*-$C_6F_2H_3$)), 6.95 (m, 3H, P*Ph*Me$_2$), 6.99 (m, 1H, Rh(*p*-$C_6F_2H_3$)), 7.66 (m, 2H, P*Ph*Me$_2$). $^{19}F\{^1H\}$ NMR (C_6D_6): δ –17.56 (m, 1 F*ortho*), –24.86 (m, 1 F*ortho*). $^{31}P\{^1H\}$ NMR (C_6D_6): δ 11.81 (dm, $^1J_{RhP}$ = 137.4 Hz).

For Tp′Rh(2,5-$C_6F_2H_3$)H(PPhMe_2) (9g). Yield, 22.5 mg, 91%. Colorless single crystals of **9g** suitable for X-ray crystallographic analysis were grown from hexane at –20 °C. **9g**: ^1H NMR (C_6D_6): δ –15.69 (ddd, $^1J_{RhH}$ = 20.4 Hz, $^2J_{PH}$ = 26.9 Hz, $^4J_{FH}$ = 11.2 Hz, 1H, RhH), 1.29 (d, $^2J_{PH}$ = 8.8 Hz, 3H, PPh*Me*$_2$), 1.65 (s, 3H, pzCH_3), 1.79 (s, 3H, pzCH_3), 1.82 (d, $^2J_{PH}$ = 9.2 Hz, 3H, PPh*Me*$_2$), 1.91 (s, 3H, pzCH_3), 2.06 (s, 3H, pzCH_3), 2.22 (s, 3H, pzCH_3), 2.34 (s, 3H, pzCH_3), 5.42 (s, 1H, pzH), 5.44 (s, 1H, pzH), 5.83 (s, 1H, pzH), 6.55 (m, 1H, $C_6F_2H_3$), 6.72 (m, 1H, $C_6F_2H_3$), 6.92 (m, 3H, P*Ph*Me$_2$), 6.93 (m, 1H, $C_6F_2H_3$), 7.65 (m, 2H, P*Ph*Me$_2$). $^{13}C\{^1H\}$ NMR (C_6D_6): δ 12.75, 13.05, 13.17, 14.90, 16.21, 16.26 (s, pzCH_3), 18.27 (d, $^1J_{PC}$ = 30.5 Hz, PPh*Me*$_2$), 22.62 (dm, $^1J_{PC}$ = 35.2 Hz, PPh*Me*$_2$), 106.47 (d, $^4J_{PC}$ = 3.3 Hz, pzCH), 106.65 (s, pzCH), 107.52 (s, pzCH), 109.87 (dd, $^2J_{FC}$ = 24.4 Hz, $^3J_{FC}$ = 9.2 Hz, CH, *m*-$C_6F_2H_3$),

112.61 (dd, $^2J_{FC}$ = 35.7 Hz, $^3J_{FC}$ = 8.4 Hz, CH, *p*-$C_6F_2H_3$), 129.74 (s, P*Ph*Me$_2$), 131.77 (dd, $^1J_{PC}$ = 10.2 Hz, $^2J_{RhC}$ = 2.6 Hz, P*Ph*Me$_2$), 138.23 (s, P*Ph*Me$_2$), 138.65 (s, P*Ph*Me$_2$), 141.59 (dddd, br, $^1J_{RhC}$ = 42.9 Hz, C, *ipso*-$C_6F_2H_3$), 143.21 (d, $^3J_{PC}$ = 2.4 Hz, pzCq), 144.07 (s, pzCq), 144.52 (s, pzCq), 150.13 (s, pzCq), 150.77 (s, pzCq), 151.15 (s, pzCq), 157.85 (d, $^1J_{FC}$ = 240.0 Hz, CF, *m*-$C_6F_2H_3$), 165.56 (d, $^1J_{FC}$ = 221.3 Hz, CF, *o*-$C_6F_2H_3$). The signal assignable to the *ortho* CH of 2,5-$C_6F_2H_3$ group was not detected probably because of the overlap with solvent peaks. $^{19}F\{^1H\}$ NMR (C_6D_6): δ –27.25 (m, 1 F*ortho*), –60.36 (m, 1 F*meta*). $^{31}P\{^1H\}$ NMR (C_6D_6): δ 11.63 (ddd, $^1J_{RhP}$ = 140.3 Hz, $^4J_{FP}$ = 16.3, 6.2 Hz). Anal. Calcd for $C_{29}H_{37}BF_2N_6PRh$: C, 53.39; H, 5.72; N, 12.88. Found: C, 53.15; H, 5.52; N, 12.65.

Tp′Rh(2-C_6FH_4)H(PPhMe$_2$) (9h). Photolysis resulted in the formation of **9h** with the isomers Tp′Rh(3-C_6FH_4)H(PPhMe$_2$) and Tp′Rh(4-C_6FH_4)H(PPhMe$_2$), and **7**, as judged by ^{1}H NMR spectroscopy. Heating at 120 °C for 1 h in C_6FH_5 solution resulted in the quantitative formation of **9h**. Yield, 20.5 mg, 85%. Colorless single crystals of **9h** suitable for X-ray crystallographic analysis were grown from hexane at –20 °C. **9h**: ^{1}H NMR (C_6D_6): δ –15.79 (ddd, $^1J_{RhH}$ = 20.2 Hz, $^2J_{PH}$ = 27.4 Hz, $^4J_{FH}$ = 10.8 Hz, 1H, RhH), 1.35 (d, $^2J_{PH}$ = 9.2 Hz, 3H, PPh*Me*$_2$), 1.67 (s, 3H, pzCH$_3$), 1.77 (s, 3H, pzCH$_3$), 1.88 (d, $^2J_{PH}$ = 8.8 Hz, 3H, PPh*Me*$_2$), 1.92 (s, 3H, pzCH$_3$), 2.12 (s, 3H, pzCH$_3$), 2.23 (s, 3H, pzCH$_3$), 2.41 (s, 3H, pzCH$_3$), 5.45 (s, 1H, pzH), 5.46 (s, 1H, pzH), 5.87 (s, 1H, pzH), 6.60 (m, 1H, C_6FH_4), 6.88 (m, 1H, C_6FH_4), 6.93 (m, 3H, P*Ph*Me$_2$), 6.97 (m, 1H, C_6FH_4), 7.19 (m, 1H, C_6FH_4), 7.70 (m, 2H, P*Ph*Me$_2$). $^{13}C\{^1H\}$ NMR (C_6D_6): δ 12.76, 13.06, 13.21, 14.90, 16.30, 16.36 (s, pzCH$_3$), 18.53 (d, $^1J_{PC}$ = 30.2 Hz, PPh*Me*$_2$), 23.43 (dm, $^1J_{PC}$ = 29.9 Hz, PPh*Me*$_2$), 106.34 (d, $^4J_{PC}$ = 3.3 Hz, pzCH), 106.59 (s, pzCH), 107.33 (s, pzCH), 112.76 (d, $^2J_{FC}$ = 31.7 Hz, CH, *m*-C_6FH_4), 122.30 (s, CH, *m*-C_6FH_4), 123.89 (d, $^3J_{FC}$ = 8.1 Hz, CH, *p*-C_6FH_4), 129.64 (s, P*Ph*Me$_2$), 131.88 (dd, $^1J_{PC}$ = 10.1 Hz, $^2J_{RhC}$ = 2.7 Hz, P*Ph*Me$_2$), 141.59 (dddd, br, $^1J_{RhC}$ = 41.6 Hz, C, *ipso*-C_6FH_4), 138.54 (s, P*Ph*Me$_2$), 138.96 (s, P*Ph*Me$_2$), 142.97 (d, $^3J_{PC}$ = 2.4 Hz, pzCq), 143.42 (d, $^3J_{FC}$ = 14.0 Hz, CH, *o*-C_6FH_4), 143.80 (s, pzCq), 144.35 (s, pzCq), 150.25 (s, pzCq), 149.88 (s, pzCq), 151.08 (s, pzCq), 169.62 (d, $^1J_{FC}$ = 233.9 Hz, CF, *o*-C_6FH_4). $^{19}F\{^1H\}$ NMR (C_6D_6): δ –19.86 (m, 1 F*ortho*). $^{31}P\{^1H\}$ NMR (C_6D_6): δ 12.06 (dm, $^1J_{RhP}$ = 133.7 Hz). Anal. Calcd for $C_{29}H_{38}BFN_6PRh$: C, 54.91; H, 6.04; N, 13.25. Found: C, 54.68; H, 5.96; N, 13.24.

Kinetics of reductive elimination reactions of Ar^{F}H from the complexes 9a–e, 9g–h and 6

A resealable 5 mm NMR tube containing the complexes **9a–e**, **9g–9h** or **6** (6–8 mg) was charged with 0.7 mL of THF-d_8 followed by 0.5 μL of hexamethyldisiloxane added as an internal standard. The sample was placed in a oil bath set to 120 °C. NMR spectra were recorded at regular intervals by ^{1}H NMR spectroscopy. Kinetic analyses were performed by integration of the decreasing hydride resonance relative to the signal for hexamethyldisiloxane. For all of the complexes, the eliminations did not go to completion and were fit to an approach to the equilibrium using the KINSIM/FITSIM[29] software package to determine the rate constant of reductive elimination of the corresponding fluoroarenes. For compound **6**, an Eyring plot was used to extrapolate the rate of the reaction at 120 °C using rate data taken at 60, 70, 80, and 90 °C (see Supporting Information‡).

X-ray data collection of the complexes, 1, 2-d_6, 3a, 3b, 3g, 5, 7, 9a, 9b, 9c, 9d, 9e and 9g

All crystals were placed onto the tip of a 0.1 mm diameter glass capillary tube or fiber and mounted on a Bruker SMART APEX II CCD Platform diffractometer for a data collection at 100.0(1) K except for **9c** (173(1) K).[34] A preliminary set of cell constants and an orientation matrix were calculated from reflections harvested from three orthogonal wedges of reciprocal space. The full data collection was carried out using Mo-Kα radiation (graphite monochromator). The intensity data were corrected for absorption.[35] The structures were solved using SIR97[36] and refined using SHELXL-97.[37] Space groups were determined based on systematic absences and intensity statistics. Except in structures **3a** and **3b**, hydride and deuteride ligands were found from the difference Fourier map, and their positions and isotropic displacement parameters were refined independently from those of rhodium atoms. These are represented with thermal spheres (50% or 30% probability density) in the figures. In structure **3a**, the position of the hydride ligand was refined independently from that of rhodium atom, but its isotropic displacement parameter was refined relatively (U_{iso}[H] = 2*U_{eq}[Rh]). Due to the severe disorder in **3b**, the hydride ligand was neither located nor placed; however, it was included in the molecular formula. All other hydrogen atoms were placed geometrically and refined with relative isotropic displacement parameters.

Crystallographic data for 1

$C_{18}H_{33}BN_6PRh$ MW = 478.19; crystal system, Triclinic; space group, $P\bar{1}$; a = 10.0429(15), b = 11.5505(18) Å, c = 11.6084(18) Å; α = 62.668(2)°; β = 80.643(3)°; γ = 66.913(3)°; V = 1100.2(3) Å^3; Z = 2; D_c = 1.443 Mg m^{-3}; μ = 0.864 mm^{-1}; 24361 reflections measured, 9947 unique (R(int) = 0.0315), 261 parameters, $R_1(I > 2\sigma(I))$ = 0.0302; wR_2 (all data) = 0.0762; GOF = 1.037.

Crystallographic data for 2-d_6

$C_{24}H_{31}BD_6N_6PRh$ MW = 560.32; crystal system, Monoclinic; space group, Cc; a = 12.8303(11), b = 15.7867(13) Å, c = 14.1339(17) Å; α = 90°; β = 111.057(1)°; γ = 90°; V = 2671.6(5) Å^3; Z = 4; D_c = 1.393 Mg m^{-3}; μ = 0.722 mm^{-1}; 32307 reflections measured, 14040 unique (R(int) = 0.0292), 315 parameters, $R_1(I > 2\sigma(I))$ = 0.0272; wR_2 (all data) = 0.0592; GOF = 1.013.

Crystallographic data for 3a·0.5(C_6H_{14})

$C_{27}H_{39}BF_5N_6PRh$ MW = 687.33; crystal system, Monoclinic; space group, $P2_1/n$; a = 8.6504(13), b = 33.930(5) Å, c = 20.878(3) Å; α = 90°; β = 100.671(2)°; γ = 90°; V = 6021.8(15) Å^3; Z = 8; D_c = 1.516 Mg m^{-3}; μ = 0.680 mm^{-1}; 74170 reflections measured, 12307 unique (R(int) = 0.1197), 787 parameters, $R_1(I > 2\sigma(I))$ = 0.0802; wR_2 (all data) = 0.1985; GOF = 1.051.

Crystallographic data for 3b

$C_{24}H_{33}BF_4N_6PRh$ MW = 626.25; crystal system, Orthorhombic; space group, $Pca2_1$; a = 29.063(3), b = 10.5847(12) Å, c = 17.7982(19) Å; V = 5475.0(10) Å^3; Z = 8; D_c = 1.520 Mg m^{-3}; μ = 0.735 mm^{-1}; 117833 reflections measured, 26396 unique

(R(int) = 0.1168), 906 parameters, $R_1(I > 2\sigma(I)) = 0.0646$; w$R_2$ (all data) = 0.1464; GOF = 1.014.

Structure description for 3b

The structure is the one suggested. There are two molecules in the asymmetric unit, both which are modeled as disordered over two positions. Initially each molecular disorder was refined independently, but it was found that the 85 : 15 component ratio resulted for both. Upon further examination, it was plain that the disorders had to be refined together to avoid close intermolecular contacts. The two positions of molecule one (Rh1) had only the rhodium atom in common, whereas the all atoms of molecule two (Rh2, Rh2′) were in different positions. In both cases, the two components were related by a pseudo-mirror (the disorder ratio of 85 : 15 disallows the refinement in a centrosymmetric space group).

Crystallographic data for 3g

$C_{24}H_{35}BF_2N_6PRh$ MW = 590.27; crystal system, Monoclinic; space group, $P2_1/c$; a = 10.4449(16), b = 14.597(2) Å, c = 17.499(3) Å; $\alpha = 90°$; $\beta = 92.021(3)°$; $\gamma = 90°$; $V = 266.4(7)$ Å^3; $Z = 4$; $D_c = 1.470$ Mg m^{-3}; $\mu = 0.739$ mm^{-1}; 42567 reflections measured, 8144 unique (R(int) = 0.1125), 332 parameters, $R_1(I > 2\sigma(I)) = 0.0488$; w$R_2$ (all data) = 0.1167; GOF = 0.995.

Crystallographic data for 5

$C_{23}H_{35}BN_6PRh$ MW = 540.26; crystal system, Monoclinic; space group, $P2_1/c$; a = 11.4148(12), b = 15.6111(16) Å, c = 14.8282(15) Å; $\alpha = 90°$; $\beta = 107.784(2)°$; $\gamma = 90°$; V = 2516.1(4) Å^3; $Z = 4$; $D_c = 1.426$ Mg m^{-3}; $\mu = 0.765$ mm^{-1}; 60723 reflections measured, 13296 unique (R(int) = 0.0989), 305 parameters, $R_1(I > 2\sigma(I)) = 0.0499$; w$R_2$ (all data) = 0.1064; GOF = 0.993.

Crystallographic data for 7

$C_{23}H_{33}BN_6PRh$ MW = 538.24; crystal system, Monoclinic; space group, $P2_1/n$; a = 13.600(4), b = 12.888(4) Å, c = 14.424(4) Å; $\alpha = 90°$; $\beta = 103.895(4)°$; $\gamma = 90°$; $V = 2454.0(12)$ Å^3; $Z = 4$; $D_c = 1.457$ Mg m^{-3}; $\mu = 0.784$ mm^{-1}; 42160 reflections measured, 8821 unique (R(int) = 0.1047), 301 parameters, $R_1(I > 2\sigma(I)) = 0.0776$; w$R_2$ (all data) = 0.1888; GOF = 1.127.

Crystallographic data for 9a

$C_{35}H_{48}BF_5N_6PRh$ MW = 792.48; crystal system, Triclinic; space group, $P\bar{1}$; a = 10.2069(10), b = 13.0730(13) Å, c = 15.3042(15) Å; $\alpha = 105.613(2)°$; $\beta = 108.235(2)°$; $\gamma = 101.547(2)°$; V = 1775.4(3) Å^3; $Z = 2$; $D_c = 1.482$ Mg m^{-3}; $\mu = 0.587$ mm^{-1}; 41158 reflections measured, 16867 unique (R(int) = 0.0277), 400 parameters, $R_1(I > 2\sigma(I)) = 0.0286$; w$R_2$ (all data) = 0.0742; GOF = 1.057.

Crystallographic data for 9b·C_6H_{14}

$C_{35}H_{49}BF_4N_6PRh$ MW = 774.49; crystal system, Triclinic; space group, $P\bar{1}$; a = 10.2654(11), b = 13.2828(14) Å, c = 15.0471(16) Å; $\alpha = 106.173(2)°$; $\beta = 107.854(2)°$; $\gamma = 101.522(2)°$; V = 1782.1(3) Å^3; $Z = 2$; $D_c = 1.443$ Mg m^{-3}; $\mu = 0.579$ mm^{-1}; 64752 reflections measured, 18391 unique (R(int) = 0.0362), 447 parameters, $R_1(I > 2\sigma(I)) = 0.0326$; w$R_2$ (all data) = 0.0849; GOF = 1.040.

Crystallographic data for 9c

$C_{29}H_{35}BF_4N_6PRh$ MW = 688.32; crystal system, Monoclinic; space group, $P2_1/n$; a = 11.9400(8), b = 18.7449(13) Å, c = 14.5298(10) Å; $\alpha = 90°$; $\beta = 109.712(1)°$; $\gamma = 90°$; V = 3061.4(4) Å^3; $Z = 4$; $D_c = 1.493$ Mg m^{-3}; $\mu = 0.664$ mm^{-1}; 74523 reflections measured, 16316 unique (R(int) = 0.0421), 391 parameters, $R_1(I > 2\sigma(I)) = 0.0427$; w$R_2$ (all data) = 0.1209; GOF = 0.996.

Crystallographic data for 9d

$C_{29}H_{36}BF_3N_6PRh$ MW = 670.33; crystal system, Triclinic; space group, $P\bar{1}$; a = 10.2916(14), b = 11.5263(16) Å, c = 12.4406(17) Å; $\alpha = 90.743(2)°$; $\beta = 93.433(2)°$; $\gamma = 92.065(2)°$; $V = 1472.0(3)$ Å^3; $Z = 2$; $D_c = 1.512$ Mg m^{-3}; $\mu = 0.684$ mm^{-1}; 34212 reflections measured, 13969 unique (R(int) = 0.0365), 382 parameters, $R_1(I > 2\sigma(I)) = 0.0332$; w$R_2$ (all data) = 0.0830; GOF = 1.045.

Crystallographic data for 9e

$C_{29}H_{37}BF_2N_6PRh$ MW = 652.34; crystal system, Triclinic; space group, $P\bar{1}$; a = 10.2523(9), b = 11.6983(10) Å, c = 12.3627(11) Å; $\alpha = 92.716(2)°$; $\beta = 95.959(2)°$; $\gamma = 92.041(2)°$; $V = 1471.8(2)$ Å^3; $Z = 2$; $D_c = 1.472$ Mg m^{-3}; $\mu = 0.677$ mm^{-1}; 26065 reflections measured, 9759 unique (R(int) = 0.0961), 373 parameters, $R_1(I > 2\sigma(I)) = 0.0568$; w$R_2$ (all data) = 0.1230; GOF = 0.968.

Crystallographic data for 9g

$C_{29}H_{37}BF_2N_6PRh$ MW = 652.34; crystal system, Triclinic; space group, $P\bar{1}$; a = 10.1914(10), b = 10.5164(11) Å, c = 15.794(2) Å; $\alpha = 99.310(2)°$; $\beta = 99.180(2)°$; $\gamma = 115.370(2)°$; $V = 1458.8(3)$ Å^3; $Z = 2$; $D_c = 1.485$ Mg m^{-3}; $\mu = 0.683$ mm^{-1}; 39002 reflections measured, 13918 unique (R(int) = 0.0391), 373 parameters, $R_1(I > 2\sigma(I)) = 0.0401$; w$R_2$ (all data) = 0.1029; GOF = 1.038.

Computational details

All calculations were performed with the Gaussian03 package[38] of programs with the hybrid B3PW91 functional.[39,40] The Rh atom was represented by the relativistic effective core potential (RECP) from the Stuttgart group and the associated basis set,[41] augmented by an f polarization function.[42] The phosphorus atom was treated with Dolg pseudopotential and the associated basis set[43] plus a d polarization function.[44] The remaining atoms (C, H, N, B, F) were represented by a 6-31G(d,p) basis set.[45] Full optimization of geometry was performed without any constraint, followed by analytical computation of the Hessian matrix to identify the nature of the located extrema as minima. See Supporting Information for details.‡

Acknowledgements

We would like to acknowledge the U.S. Department of Energy Sciences (FG02-86ER13569) for their support of this work. T.T. thanks the Japanese Society for Promotion of Science for a postdoctoral fellowship. OE and EC thank the CNRS and

the Ministère de l'Education Supérieure et de la Recherche for funding. We also that Prof. Robin Perutz for early suggesting regarding the value of making these quantitative measurements.

References

1 G. W. Parshall, *Acc. Chem. Res.*, 1975, **8**, 113; R. H Crabtree, *Chem. Rev.*, 1985, **85**, 245; W. D. Jones and F. J. Feher, *Acc. Chem. Res.*, 1989, **22**, 91; B. A. Arndsten, R. G. Bergman, T. A. Mobley and T. H. Peterson, *Acc. Chem. Res.*, 1995, **28**, 154; A. E Shilov and G. B. Shul'pin, *Chem. Rev.*, 1997, **97**, 2879; W. D. Jones, *Top. Organomet. Chem.*, 1999, **3**, 9; V. Ritleng, C. Sirlin and M. Pfeffer, *Chem. Rev.*, 2002, **102**, 1731; W. D. Jones, *Acc. Chem. Res.*, 2003, **36**, 140; W. D. Jones, *Inorg. Chem.*, 2005, **44**, 4475; E. Clot, O. Eisenstein and W. D. Jones, *Proc. Natl. Acad. Sci. U. S. A.*, 2007, **104**, 6939; A. J. Vetter, R. D. Rieth and W. D. Jones, *Proc. Natl. Acad. Sci. U. S. A.*, 2007, **104**, 6957; M. T. Whited and R. H. Grubbs, *Acc. Chem. Res.*, 2009, **42**, 1607. See also a special issue reviewing selective C–H activation: R. H. Crabtree, *Chem. Rev.*, 2010, **110**, 575.

2 M. Lin and A. Sen, *Nature*, 1994, **368**, 613; L.-C. Kao, A. C. Hutson and A. Sen, *J. Am. Chem. Soc.*, 1991, **113**, 700; A. Sen, E. Gretz, T. F. Oliver and Z. Jiang, *New J. Chem.*, 1989, **13**, 755; A. Sen, *Acc. Chem. Res.*, 1988, **21**, 421; C. P. Schaller and P. T. Wolczanski, *Inorg. Chem.*, 1993, **32**, 131; G. A. Luinstra, J. A. Labinger and J. E. Bercaw, *J. Am. Chem. Soc.*, 1993, **115**, 3004; J. A. Labinger, A. M. Herring, D. K. Lyon, G. A. Luinstra, J. E. Bercaw, I. T. Horváth and K. Eller, *Organometallics*, 1993, **12**, 895; R. A. Periana, D. J. Taube, E. R. Evitt, D. G. Loffler, P. R. Wentrcek, G. Voss and T. Masuda, *Science*, 1993, **259**, 340.

3 C. L. Hill, *Activation and Functionalization of Alkanes*, Wiley: New York, 1989; J. A. Davies, P. L. Watson, J. F. Liebman and A. Greenberg, *Selective Hydrocarbon Activation*, VCH Publishers, Inc.: New York, 1990; P. Burger and R. G. Bergman, *J. Am. Chem. Soc.*, 1993, **115**, 10462; B. A. Arndtsen and R. G. Bergman, *Science*, 1995, **270**, 1970; H. F. Luecke, B. A. Arndtsen, P. Burger and R. G. Bergman, *J. Am. Chem. Soc.*, 1996, **118**, 2517; M. W. Holtcamp, J. A. Labinger and J. E. Bercaw, *J. Am. Chem. Soc.*, 1997, **119**, 848; D. L. Strout, S. Zaric, S. Niu and M. B. Hall, *J. Am. Chem. Soc.*, 1996, **118**, 6068.

4 W. D. Jones and F. J. Feher, *J. Am. Chem. Soc.*, 1984, **106**, 1650.

5 C. K. Ghosh and W. A. G. Graham, *J. Am. Chem. Soc.*, 1987, **109**, 4726.

6 W. D. Jones and E. T. Hessell, *J. Am. Chem. Soc.*, 1993, **115**, 554.

7 W. D. Jones and L. Dong, *J. Am. Chem. Soc.*, 1989, **111**, 8722; W. D. Jones and V. L. Kuykendall, *Inorg. Chem.*, 1991, **30**, 2615; W. D. Jones and E. T. Hessell, *J. Am. Chem. Soc.*, 1992, **114**, 6087; D. D. Wick and W. D. Jones, *Organometallics*, 1999, **18**, 495; T. O. Northcutt, D. D. Wick, A. J. Vetter and W. D. Jones, *J. Am. Chem. Soc.*, 2001, **123**, 7257; A. J. Vetter, R. R. Rieth and W. D. Jones, *J. Am. Chem. Soc.*, 2005, **127**, 12315; M. E. Evans, T. Li, A. J. Vetter, R. D. Rieth and W. D. Jones, *J. Org. Chem.*, 2009, **74**, 6907.

8 J. L. Bennett and P. T. Wolczanski, *J. Am. Chem. Soc.*, 1994, **116**, 2179.

9 J. L. Bennett and P. T. Wolczanski, *J. Am. Chem. Soc.*, 1997, **119**, 10696.

10 H. E. Bryndza, L. K. Fong, R. A. Paciello, W. Tam and E. Bercaw, *J. Am. Chem. Soc.*, 1987, **109**, 1444.

11 P. L. Holland, R. A. Andersen, R. G. Bergman, J. Huang and S. P. Nolan, *J. Am. Chem. Soc.*, 1997, **119**, 12800.

12 L. E. Schock and T. J. Marks, *J. Am. Chem. Soc.*, 1988, **110**, 7701.

13 W. A. King, S. Di Bella, A. Gulino, G. Lanza, I. L. Fragalà, C. L. Stern and T. J. Marks, *J. Am. Chem. Soc.*, 1999, **121**, 355.

14 C. D. Hoff, *Prog. Inorg. Chem.*, 1992, **40**, 503.

15 T. Ishiyama and N. Miyaura, *J. Organomet. Chem.*, 2003, **78**, 1369; T. Ishiyama and N. Miyaura, *Pure Appl. Chem.*, 2006, **680**, 3; J. Y. Jian-Yang Cho, M. K. Tse, D. Holmes, R. E. Maleczka Jr and M. R. Smith III, *Science*, 2002, **295**, 302; D. N. Coventry, A. S. Batsanov, A. E. Goeta, J. A. K. Howard, T. B. Marder and R. N. Perutz, *Chem. Commun.*, 2005, 2172; J. M. Murphy, C. C. Tzschucke and J. F. Hartwig, *Org. Lett.*, 2007, **9**, 757; C. C. Tzschucke, J. M. Murphy and J. F. Hartwig, *Org. Lett.*, 2007, **9**, 761; A. R. Dick and M. S. Sanford, *Tetrahedron*, 2006, **62**, 2439.

16 D Alberico, M. E. Scott and M Lautens, *Chem. Rev.*, 2007, **107**, 174; J. P. Wolfe and S. L. Buchwald, *Angew. Chem., Int. Ed.*, 1999, **38**, 2413; J. P. Wolfe, R. A. Singer, B. H. Yang and S. L. Buchwald, *J. Am. Chem. Soc.*, 1999, **121**, 9550; A. F. Littke and G. C. Fu, *Angew. Chem., Int. Ed.*, 2002, **41**, 4176; F. Bellina, S. Cauteruccio and R. Rossi, *Eur. J. Org. Chem.*, 2006, 1379.

17 L.-C. Campeau and K. Fagnou, *Chem. Commun.*, 2006, 1253; M. Lafrance, C. N. Rowley, T. K. Woo and K. Fagnou, *J. Am. Chem. Soc.*, 2006, **128**, 8754; M. Lafrance, D. Shore and K. Fagnou, *Org. Lett.*, 2006, **8**, 5097.

18 Calculations on osmium and rhodium complexes showed that the barrier to oxidative addition of the C–F bond is ~24 kcalmol^{-1} higher than that of C–H bond. See, R. Bosque, E. Clot, S. Fantacci, F. Maseras, O. Eisenstein, R. N. Perutz, K. B. Renkema and K. G. Caulton, *J. Am. Chem. Soc.*, 1998, **120**, 12634.

19 E. Clot, M. Besora, F. Maseras, C. Mégret, O. Eisenstein, B. Oelckers and R. N. Perutz, *Chem. Commun.*, 2003, 490.

20 L. Cronin, C. L. Higgitt, R. Karch and R. N. Perutz, *Organometallics*, 1997, **16**, 4920; M Reinhold, J. E. McGrady and R. N. Perutz, *J. Am. Chem. Soc.*, 2004, **126**, 5268; T Schaub, P Fischer, A. Steffen, T. Braun, U. Radius and A Mix, *J. Am. Chem. Soc.*, 2008, **130**, 9304; S. A. Johnson, C. W. Huff, F. Mustafa and M. Saliba, *J. Am. Chem. Soc.*, 2008, **130**, 17278; I. Bach, K. R. Pörschke, R. Goddard, C. Kopiske, C. Krüger, A. Rufińska and K. Seevogel, *Organometallics*, 1996, **15**, 4959.

21 E. Clot, B. Oelckers, A. H. Klahn, O. Eisenstein and R. N. Perutz, *Dalton Trans.*, 2003, 4065.

22 E. Clot, C. Mégret, O. Eisenstein and R. N. Perutz, *J. Am. Chem. Soc.*, 2009, **131**, 7817.

23 M. E. Evans, C. L. Burke, S. Yaibuathes, E. Clot, O. Eisenstein and W. D. Jones, *J. Am. Chem. Soc.*, 2009, **131**, 13464.

24 M. Paneque, S. Taboada and E. Carmona, *Organometallics*, 1996, **15**, 2678; M. Paneque, P. J. Pérez, A. Pizzano, M. L. Poveda, S. Taboada, M. Trujillo and E. Carmona, *Organometallics*, 1999, **18**, 4304; M. C. Nicasio, M. Paneque, P. J. Pérez, A. Pizzano, M. L. Poveda, L. Rey, S. Sirol, S. Taboada, M. Trujillo, A. Monge, C. Ruiz and E. Carmona, *Inorg. Chem.*, 2000, **39**, 180.

25 D. D. Wick and W. D. Jones, *Inorg. Chim. Acta*, 2009, **362**, 4416.

26 D. D. Wick and W. D. Jones, *Inorg. Chem.*, 1997, **36**, 2723.

27 M. Paneque, S. Sirol, S. Taboada, M. Trujillo, E. Carmona, E. Gutiérrez-Puebla, M. A. Monge, C. Ruiz, F. Malbosc, C. S. Berre, P. Kalck, M. Etienne and J. C. Daran, *Chem.–Eur. J.*, 2001, **7**, 3868.

28 A related four-membered-ring phospha-rhodacycle, in which rhodium and phosphorus atoms are fused with phenyl ring on the phosphorus atom, $(PPh_3)_2Rh(k^2\text{-}C_6H_4\text{-}2\text{-}PPh_2)$ ($d_P = -54.2$ ($^1J_{RhP} = 119$ Hz)), has been reported. See, S. H. Strauss, S. E. Diamond, F. Mares and D. F. Shriver, *Inorg. Chem.*, 1978, **16**, 1974.

29 C. Frieden, *KINSIM*, Washington University School of Medicine: St. Louis, MO, 1997 http://www.biochem.wustl.edu/cflab/message.html.

30 The model used in the calculation was $TpRh(Ar^F)H(PMe_3)$. See ref. 23.

31 S. J. Trofimenko, *J. Am. Chem. Soc.*, 1967, **89**, 3165; S. J. Trofimenko, *Inorg. Synth.*, 1970, **12**, 99.

32 B. D. Catsikis and M. L. Good, *Inorg. Chem.*, 1969, **8**, 1095; B. D. Catsikis and M. L. Good, *Inorg. Nucl. Chem. Lett.*, 1968, **4**, 529.

33 O. Renn, H. Rüegger, L. M. Venanzi, J. Gallus, V. Gramlich and A Martelletti, *Inorg. Chim. Acta*, 1995, **240**, 575.

34 *APEX2*, version 2009.3-0Bruker AXS: Madison, WI, 2009.

35 G. M. Sheldrick, *SADABS*, version 2008/1; University of Göttingen: Göttingen, Germany, 2008.

36 A. Altomare, M. C. Burla, M. Camalli, G. L. Cascarano, C. Giacovazzo, A. Guagliardi, A. G. G. Moliterni, G. Polidori and R. Spagna, *SIR97: A new program for solving and refining crystal structures*Istituto di Cristallografia, CNR: Bari, Italy, 1999.

37 G. M. Sheldrick, *Acta Crystallogr., Sect. A: Found. Crystallogr.*, 2008, **64**, 112.

38 M. J. Frisch *et al.*, *Gaussian 03*, Revision C.02, Gaussian Inc Wallingford CT, 2004.

39 A. D. Becke, *J. Chem. Phys.*, 1993, **98**, 5648.

40 J. P. Perdew and Y. Wang, *Phys. Rev. B: Condens. Matter*, 1992, **45**, 13244.

41 D. Andrae, U. Häussermann, M. Dolg, H. Stoll and H. Preuss, *Theor. Chim. Acta*, 1990, **77**, 123.

42 A. W. Ehlers, M. Böhme, S. Dapprich, A. Gobbi, A. Höllwarth, V. Jonas, K. F. Köhler, R. Stegmann, A. Veldkamp and G. Frenking, *Chem. Phys. Lett.*, 1993, **208**, 111.

43 A. Bergner, M. Dolg, W. Küchle, H. Stoll and H. Preuss, *Mol. Phys.*, 1993, **80**, 1431.

44 A. Höllwarth, H. Böhme, S. Dapprich, A. W. Ehlers, A. Gobbi, V. Jonas, K. F. Köhler, R. Stegmann, A. Veldkamp and G. Frenking, *Chem. Phys. Lett.*, 1993, **208**, 237.

45 P. C. Hariharan and J. A. Pople, *Theor. Chim. Acta*, 1973, **28**, 213.